DESCRIPTION

APPARATUS AND METHOD FOR NOISE-PREDICTIVE MAXIMUM-LIKELIHOOD (NPML) DETECTION

TECHNICAL FIELD

The invention relates to data detection methods and apparatus, particularly methods and apparatus for partial-response signaling and maximum-likelihood sequence detection. It further relates to direct access storage devices (DASDs) based on these methods.

BACKGROUND OF THE INVENTION

Application of partial-response (PR) class-IV (PR4) equalization and maximum likelihood sequence detection (MLSD) has been shown in theory and practice to achieve near optimal performance at recording densities of $0.8 \leq PW50/T \leq 1.6$, where PW50 is the pulse width at the 50% amplitude point of the channel's step response and T is the duration of the channel encoded bit. A partial response maximum likelihood (PRML) system for the magnetic recording channel has been described in "A PRML system for Digital Magnetic Recording," Roy D. Cideciyan et al., IEEE Journal on Selected Areas in Communications, Vol. 10, No. 1, pp. 38 - 56, January 1992. In the US patent No. 4,786,890 a class-IV PRML channel using a run-length limited (RLL) code has also been disclosed.

At high recording densities, i.e., $PW50/T > 1.6$, the linear partial-response class-IV equalizer leads to substantial noise enhancement. As a consequence, the performance of the PRML detector suffers and may become inadequate to meet product specifications. Application of extended partial-response maximum likelihood (EPRML) detectors has been shown in theory and

practice to achieve better performance than PRML detectors in the range PW50/T > 1.6. The patent application GB-A-2286952, published on 30 August 1995, discloses a novel EPRML scheme for data detection in a direct access storage device. The novel architecture of the invention claimed therein allows for the addition of EPRML detectors to PRML channels with only minor changes to the overall channel architecture.

The optimum MLSD receiver for detecting an uncoded data sequence in the presence of intersymbol-interference (ISI) and additive Gaussian noise consists of a whitened-matched filter followed by a Viterbi detector which performs maximum likelihood sequence detection on the ISI trellis, as described by G. D. Forney in "Maximum-likelihood sequence estimation of digital sequences in the presence of intersymbol interference," IEEE Trans. Inform. Theory, Vol. IT-18, No. 3, pp. 363 - 378, May 1972. For the magnetic recording channel the state complexity of this trellis is given by 2^L where L represents the number of relevant ISI terms in the output signal of the whitened-matched filter. In the patent application WO94/29989 with title "Adaptive noise-predictive partial-response equalizing for channels with spectral nulls," filed 14 June 1993 and published 22 December 1994, and in reference "Noise predictive partial-response equalizers and applications," P. R. Chevillat et al., IEEE Conf. Records ICC'92, June 14-18 1992, pp. 0942 - 0947, it was shown that a partial-response zero forcing equalizer cascaded with a linear predictor whose coefficients have been suitably chosen, is equivalent to the whitening discrete-time prefiller of the optimum MLSD receiver. Furthermore, in the same patent application a receiver structure has been disclosed where the prediction process has been imbedded in the Viterbi detector corresponding to the partial-response trellis. The above patent application WO94/29989 is primarily concerned with wire transmission systems.

In the above patent application WO94/29989 and the article of P. R. Chevillat et al. it has been concluded that noise-prediction in conjunction with PRML improves detector performance.

It is an object of the present invention to provide a method and apparatus with improved data detection performance.

It is an object of the present invention to provide a method and apparatus for improved data detection in direct access storage devices with the purpose to overcome the performance problems in prior art schemes.

It is an object of the present invention to provide a method and apparatus to achieve higher linear storage density in direct access storage devices (DASDs).

It is another object of the present invention to provide a method and apparatus which can be employed in a conventional PRML/EPRML direct access storage device without changing the principal architecture of the electronic channel.

SUMMARY OF THE INVENTION

The above objects have been accomplished by providing an entire family of estimation detectors which can for example be used for data detection in DASDs. Some of the present detectors, which make specific use of properties of the magnetic recording channel, arise by imbedding a noise prediction/whitening process into the branch metric computation of the maximum-likelihood sequence detector and are collectively called Noise Predictive Maximum Likelihood (NPML) detectors. They furthermore comprise means for cancellation of intersymbol-interference (ISI) components by an appropriate table look-up. In contrast to the patent application WO94/29989 and the article of P. R. Chevillat et al. where the state complexity of the detector is fixed and determined by the partial-response trellis, the NPML detectors have a state complexity which is equal to 2^K, where $0 \leq K \leq L$ and L reflects the number of controlled (known) Intersymbol Interference (ISI) components introduced by the combination of PR equalizer and predictor.

The special case where K = L is equivalent to the optimum MLSD detector for the given predictor length and the special case K = 0 corresponds to a noise-predictive PR equalizer followed by a memoryless detector. For $1 \leq K < L$ the NPML detector operates on a reduced set of ISI states. At the same time, the (L-K) ISI terms (components) not represented in the state-space of the NPML detector are compensated in a decision-feedback fashion by using decisions from the path history. Thus, the NPML detectors offer a trade-off between performance and state complexity and/or length of decision-feedback and they provide a substantial gain in linear recording density over PRML and EPRML detectors. In addition, the present implementations of NPML detectors do not require multiplications in the imbedded predictor and thus allow simple random access memory (RAM) look-up implementation for ISI cancellation. Furthermore, NPML detectors generally do not exhibit quasi-catastrophic error propagation. Thus, additional increases in recording density can be achieved with higher rate run-length limited (RLL) codes by relaxing the constraints relating to the survivor path memory. Finally, besides modularity and substantial gains in performance, the NPML detectors have the important implementation advantage that they can be "piggy-backed" on existing PRML/EPRML systems. Therefore, there is no need for the development and implementation of an entirely new channel architecture which is a costly and complex task.

Also described and claimed are low complexity derivatives of the NPML detector family which offer appreciable performance gains. The respective schemes include, but are not limited to, two-state interleaved NPML detectors and cascaded noise-predictors with PRML detectors. Furthermore, derived from an NPML scheme with a single-tap predictor, a programmable 8-state NPML detector is described which is capable to operate also as a PRML or EPRML detector.

DESCRIPTION OF THE DRAWINGS AND NOTATIONS USED

The invention is described in detail below with reference to the following drawings:

FIG. 1 Shows a block diagram used to illustrate how the inventive NPML detectors fit into the existing PRML channel architecture.

FIG. 2A Shows the blocks of Figure 1 which are relevant for the present invention: the digital equalizer 22, the present NPML detector 10, and inverse precoder 23.

FIG. 2B Shows an equivalent form of the present NPML detector 10, according to the present invention.

FIG. 2C Shows another equivalent, more detailed, form of the present NPML detector 10, according to the present invention.

FIG. 2D Shows yet another equivalent form of the present NPML detector 10, according to the present invention.

FIG. 2E Shows another possible embodiment of a sequence detector with imbedded feedback, according to the present invention.

FIG. 3A Shows the noise-predictive part using a memoryless detector in cascade with a conventional PRML detector, according to the present invention.

FIG. 3B Shows another approach to realize the noise-predictive part using a memoryless detector in cascade with a conventional PRML detector, according to the present invention.

FIG. 4 Shows a block diagram to illustrate the operation of the metric update unit (MUU), for some state s_i at the time nT, according to the present invention. MMUs are major functional blocks in an NPML detector.

FIG. 5 Shows a 2-state trellis diagram.

FIG. 6 Shows an implementation of a 2-state NPML detector with a 4-tap predictor, according to the present invention.

FIG. 7 Shows a 2-state trellis (difference metric) diagram.

FIG. 8 Shows one possible way of mapping the algorithm implied by the trellis diagram in Figure 7 into hardware, where the threshold for the comparators is provided by the stored difference metric D_{n-1}.

FIG. 9 Shows a 4-state trellis diagram.

FIG. 10A-10C Shows another implementation of an NPML detector, according to the present invention (4-state, 2-tap predictor).

FIG. 11A-11C Shows another implementation of an NPML detector, according to the present invention (4-state, 4-tap predictor).

FIG. 12 Shows an 8-state trellis diagram with N=1 and K=3 (8-state, 1-tap predictor).

FIG. 13 Shows a transformed 8-state trellis diagram with N=1 and K=3 (8-state, 1-tap predictor).

FIG. 14 Shows one possible way of mapping the algorithm implied by the trellis diagram in Figure 13 into a hardware structure. The survivor path memory controlled by the select-signals S0, . . ., S7, is not shown.

FIG. 15 Shows an alternate form of implementing the functions of the 2-state NPML detector with a 4-tap predictor shown in Figure 6.

FIG. 16A-16C Shows another implementation of an NPML detector, according to the present invention (4-state, N-tap predictor).

FIG. 17A-17C Shows another implementation of an NPML detector, according to the present invention (4-state, N-tap predictor).

GENERAL DESCRIPTION

In the following the principal forms of implementation of NPML Detectors are described.

The block diagram in Figure 1 shows how the present NPML detectors 10 fit into the existing PRML channel architecture. Customer data I_n are written in the form of binary digits $a_n \in \{-1, +1\}$ by write head 15 on the disk 11 after being encoded in an encoder 12 by a rate-8/9 RLL code, serialized in a serializer 13 and precoded in a precoder 14 by a $1/(1 \oplus D^2)$ operation where D is the unit delay operator. When retrieving the customer data from said disk 11, an analog signal r(t) is generated by the read head 15 and provided at the read-head's output. This signal r(t) is then applied via the arm electronics 16 to a variable-gain amplifier (VGA) circuit 17. The output signal of the VGA circuit 17 is first low-pass filtered using an analog low-pass filter 18 (LPF) and then converted to a digital form x_n by an analog-to-digital (A/D) converter 19. The functions of the A/D converter 19 and VGA unit 17 are controlled by the timing recovery and gain control loops 20 and 21, respectively. The analog

low-pass filter 18 is preferably a filter which boosts the higher frequencies to avoid saturation of the A/D converter 19. The digital samples x_n at the output of the A/D converter 19 (line labeled A in Figure 1) are first shaped to PR4 signal samples by the digital equalizer 22 (line labeled B in Figure 1) and are then passed on to the inventive NPML detector in the form of digital samples y_n. After inverse precoding by means of a precoder 23 performing a $(1 \oplus D^2)$ operation, the output data of the NPML detector 10 (i.e. the final decisions; line labeled C in Figure 1) are fed via a deserializer 24 to a decoder 25 for the rate-8/9 RLL code which delivers the retrieved customer data $\hat{i}_{n-d}$. The inverse precoder function following the NPML detector in Figure 1 can be a separate functional block (as shown) or it can be imbedded in the trellis (survivor path memory) of the detector. Figure 2A shows the blocks in Figure 1 which are relevant for the present invention: the digital equalizer 22, the NPML detector 10, and the inverse precoder 23.

Generally, the coefficients of the digital equalizer 22 can be optimized so that the overall transfer function, including the head/disk-medium characteristics and the analog LPF 18, closely matches any desired system polynomial of the generalized partial-response form $f(D) = (1 + f_1D^1 + \ldots + f_nD^n)$ where the coefficients f can be arbitrary real numbers. For example, the partial-response (PR) polynomial for class-4 PR systems (PR4) is $f(D) = (1 - D^2)$. Similarly, the polynomial for extended partial-response class-4 (EPR4) systems is $f(D) = (1 - D^2)(1 + D) = (1 + D - D^2 - D^3)$. A further example is $f(D) = (1 - 0.1D - 0.9D^2)$.

Figure 2B shows the basic structure of the NPML detector 10 in the form of a prediction error filter 41 cascaded with a sequence detector (SD) with imbedded feedback (FB) 30.

In the sequel we use PR4- equalized signals y_n (Line B in Figure 2B), however, the inventive scheme can be applied to any shaping performed by the equalizer 22 in Figures 2A and 2B.

Figures 2C and 2D show two equivalent forms of NPML detectors, according to the present invention. Its basic principle can be explained as follows. Let y_n be the output of the PR4 digital equalizer (line labeled B in Figures 1, 2C and 2D). This output then consists of a PR4 data signal and colored noise (colored interference components), i.e.,

$$y_n = a_n - a_{n-2} + w_n \tag{1}$$

where $a_n \in \{-1, +1\}$ denotes the encoded/precoded data sequence written on the magnetic medium with a rate 1/T and w_n represents the colored noise sequence at the output of the digital equalizer 22. The power of the colored noise component (colored interference component) can be reduced by noise prediction. If $p(D) = (p_1D^1 + p_2D^2 + \ldots + p_ND^N)$ denotes the transfer polynomial, or equivalently $E(D) = 1 - P(D)$ denotes the transfer polynomial of the prediction error filter, of the N-tap minimum mean-square (MMSE) predictor of the noise sample w_n then the signal

$$\begin{aligned} e_n &= w_n - \hat{w}_n = \\ &w_n - \sum_{i=1}^{N} w_{n-i}\, p_i = \\ &= (y_n - a_n + a_{n-2}) - \sum_{i=1}^{N} (y_{n-i} - a_{n-i} + a_{n-i-2})\, p_i \end{aligned} \tag{2}$$

represents the prediction error or equivalently the whitened noise component of the PR4-equalized output signal y_n. Reliable operation of the prediction/whitening process is possible by using decisions from the path history associated with each state which is available in a sequence (Viterbi) detector. In that sense, NPML detectors are MLSD detectors for (PR) signals with imbedded prediction or equivalently imbedded feedback.

In view of (1) and (2) the branch metric of the NPML detector 10 for PR4-equalized samples corresponding to a transition from state s_j to state s_k takes the form

$$\lambda(s_j, s_k) = \left| y_n - \sum_{i=1}^{N} (y_{n-i} - a_{n-i}(s_j) + a_{n-i-2}(s_j))\, p_i - a_n + a_{n-2} \right|^2 \quad (3)$$

where the terms $a_{n-i}(s_j)$, $a_{n-i-2}(s_j)$ represent past decisions taken from the path history associated with state s_j and a_n, a_{n-2} are determined by the hypothesized state transition $s_j \rightarrow s_k$. Clearly, the noise prediction process appears explicitly in the branch metric computation of the Viterbi algorithm implementing the NPML detector. Furthermore, it can be seen that by setting the predictor coefficients p_i equal to zero, the branch metric in (3) becomes the branch metric of the 4-state PRML detector.

The branch metric in (3) can also be written as

$$\lambda(s_j, s_k) = \left| y_n - \sum_{i=1}^{N} y_{n-i} p_i + \sum_{i=1}^{N} (a_{n-i}(s_j) - a_{n-i-2}(s_j)) p_i - a_n + a_{n-2} \right|^2 \quad (4)$$

By noticing that the first sum in (4) is state independent, and after some rearrangement of the remaining terms, the equivalent branch metric is obtained as

$$\lambda(s_j, s_k) = \left| z_n + \sum_{i=K+1}^{N+2} a_{n-i}(s_j) g_i + \sum_{i=1}^{K} a_{n-i} g_i - a_n \right|^2 \quad (5)$$

where the signal sample $z_n = y_n - \sum_{i=1}^{N} y_{n-i} p_i$ is the output of the prediction error filter 41, shown in the equivalent NPML implementation of Figure 2C, and

$\{g_i, i = 1,2, \ldots, N+2\}$ are the coefficients of the imbedded feedback filter 42 (FIR: finite impulse response or RAM-based filter) in Figure 2C. It can be shown that the coefficients $\{g_i, i = 1,2, \ldots, N+2\}$ introduced in (5) are the coefficients of the polynomial

$g(D) = (+1 - g_1D^1 - g_2D^2 - \cdots - g_{N+2}D^{N+2}) = (1 - D^2)(1 - P(D)) = (1 - D^2)E(D)$.

The effective ISI memory L of the PR4-based NPML system is thus $L = N+2$. The symbols $a_{n-i}(s_j)$ in the first summation term of (5) represent past decisions taken from the path history associated with state s_j, whereas the symbols a_{n-i} in the second summation term of (5) represent state information. Clearly, by increasing K we effectively increase the number of states of the NPML detector and decrease the length of the imbedded decision feedback. Conversely, by decreasing K the number of states is decreased at the expense of increasing the length of the imbedded decision feedback. Thus, the emerging family of NPML detectors, in accordance with the present invention, offers a trade-off between state complexity and length of imbedded decision feedback.

The two equivalent implementations of the NPML detector 10 shown in Figure 2C and 2D, respectively, require no change of the signal processing blocks, i.e., VGA 17, analog LPF 18, digital equalizer 22, timing recovery and gain control loops 20 and 21, of the current PRML/EPRML channel architecture used by IBM and others. Any member of the family of NPML detectors according to the present invention can either replace the PRML/EPRML detector or operate concurrently with it.

A third possible implementation of an NPML scheme in the form of a filter cascaded with a sequence detector with imbedded feedback is shown in Figure 2E. In this case the combination of digital equalizer 22 and prediction error filter 41 (see Figure 2B) is replaced by a single finite-impulse response filter designated as FIR1 51. Input to the filter FIR1 51 now are the unequalized samples x_n at the output of the A/D converter 19 (line labeled A in Figure 1 and Figure 2E). The filter FIR1 51 has the property to whiten the noise and introduce a controlled amount of ISI in the signal samples z_n at its

output. The coefficients of the feedback filter (FIR2 or RAM 52) are then used in the branch metric computation of the sequence detector with imbedded feedback in the same way described above. Thus, the branch metric takes the form

$$\lambda(s_j, s_k) = \left| z_n + \sum_{i=K+1}^{N+2} a_{n-i}(s_j) b_i + \sum_{i=1}^{K} a_{n-i} b_i - a_n \right|^2 \qquad (6)$$

where z_n is the output of FIR1 51 and $\{b_i, i = 1,2,\ldots,N-2\}$ is the set of coefficients of the filter FIR2 52. Note that expressions (5) and (6) are essentially the same. It can be shown that for infinitely long filters the three alternative implementations of sequence detection with imbedded feedback, shown in Figures 2A - 2E, are equivalent.

It should be understood that the NPML principles described hereinabove can be applied to any form of system polynomial f(D). In the sequel, however, only the PR class-IV polynomial (PR4) will be considered as the target polynomial.

Performance and Preferred Parameters for NPML Detectors Used in DASD's:

The error performance of a magnetic recording system employing NPML detection has been studied by computer simulations in order to determine the appropriate parameters N (number of predictor coefficients) and K (length of detector memory defining the number of detector states 2^K) to be used in a practical system. In particular, the cases described in this document for N=1, N=2, and N=4 predictor coefficients lead to preferred NPML detectors.

Two low-complexity derivatives of the NPML detector family have also been investigated. Both schemes, like the entire family of NPML detectors, require no change of the signal processing parts of the current PRML channel architecture (see also Figure 1). Figure 3A shows the noise-predictive part using a memoryless detector in cascade with a conventional PRML detector.

The colored noise component of the PR4-equalized signal (line labeled B in Figure 1 and 3A) is first whitened by a predictor. Note that instead of imbedding the predictor into the MLSD process, a 3-level (+2, 0, -2) memoryless detector provides the (tentative) PR4 (signal sample) decisions needed for the whitening process. The PR4-equalized samples corrupted with the whitened noise components are then fed to a conventional PRML detector and inverse precoder to obtain improved final decisions. Figure 3B is an equivalent form of the scheme in Figure 3A similar to the equivalent forms in Figure 2C and 2D, respectively.

The second low-complexity NPML detector scheme is based on the fact that PR4 sequences can be viewed as two independent, interleaved dicode sequences with polynomial $(1 - D')$, where D' refers to a delay of 2T. In this case each dicode sequence at the output of the digital equalizer (line labeled B in Figures 1, 2C, and 2D) can be described by a 2-state trellis. The Viterbi algorithm, operating separately on each of these 2-state interleaved trellises, will use the branch metrics given in (3) or (5) where the time indices are either even or odd. For example, while the Viterbi algorithm operates on the even trellis, the time indices of the branch metric expression (3) or (5) will be even whereas the contribution of the odd past decisions in whitening the noise will come from the path memory with the best metric of the odd trellis.

A further suboptimal scheme is to find the state with the best metric, compute the predictor output using the decisions from the survivor path corresponding to this best state, and applying it as a feedback term in the metric update computations for all states. This approach has the advantage that only a single RAM is needed.

Concept of NPML Detectors with Nonlinear Predictors:

The NPML concept described herein is also applicable when the noise predictor has certain nonlinear characteristics and/or the computation of the predictor coefficients is based on a different noise model.

The present NPML architecture allows for great flexibility in optimizing the noise predictor function with respect to various kinds of random noise which occur in a practical target system. For example, only a portion of the total noise in hard disk drives is adequately modelled by additive white Gaussian noise (AWGN). Besides AWGN, the total noise includes other noise sources, such as signal-dependent disk noise, noise due to texture scratches, and so forth. In addition, to a certain extent coherent interference, such as clock and/or adjacent track signals, may also exist in the analog readback signal.

Because the NPML concept allows, in effect, the transfer function for the signal portion of the input to be different than that for the noise and other interference components also present in the signal, the predictor may be optimized to minimize signal disturbances due to any type of corruptive source. Conventional detectors (such as PRML and EPRML detectors, etc.) are only optimized to the extent that the signal disturbance at the detector input is additive, random, uncorrelated and Gaussian. This is often a poor approximation in practical DASD systems; thus, using a linear predictor and/or computing the predictor coefficients based on this idealistic noise model may not lead to optimal solutions in situations where this assumption is poorly matched.

In hard disk drives, both AWGN and so-called "disk noise" are dominant sources of readback signal corruption. In the following, an example is given for a linear noise predictor with four coefficients (N=4) where the coefficients have been computed by incorporating AWGN as well as disk noise in the noise statistics. A simple model of disk noise is the so-called "transition jitter model" wherein the deviation of each written transition from its nominal location is a random variable. The effective SNR achieved at the input of a PRML detector is 15.4dB and at the input of a 64-state NPML detector 18.9dB for AWGN alone for a channel operating at PW50/T = 3. In case of AWGN combined with disk noise (transition jitter) the effective SNR at the input of a PRML detector is 12.7dB and at the input of a 64-state NPML detector 15.5dB for a channel operating at PW50/T = 3. It is interesting to note that the NPML

detector is able to adapt the predictor coefficients to different noise statistics and thus to maintain an SNR margin of 2.8-3.5dB over PRML. Although this example uses a 4-tap linear noise predictor for NPML, this technique and its benefits is herein claimed for all possible types of noise predictors, including nonlinear predictors.

Examples of Preferred Embodiments of NPML Detectors:

The preferred form of implementation of an NPML detector within a PRML system is the one given in Figure 2C. More details on this embodiment of an NPML detector 10 are given in this section. Figure 4 illustrates the operation of a major functional block in an NPML detector according to Figure 2C - the metric update unit (MUU) 68 shown here for state s_k at time nT. Figure 4 illustrates the required time relations between inputs and outputs of the various functional blocks. A separate MUU function must be provided for each hypothesized state s_k, $k = 1, 2, \ldots, 2^K$, where $K \in \{1, 2, \ldots, L\}$ and L is the number of controlled ISI terms, e.g. for PR4 $L = N + 2$. In high-performance DASDs parallel MUU hardware must be provided for each state to meet the data throughput requirements; in principle, however, hardware could be shared if speed constraints permit. Furthermore, it is assumed here and hereafter that the survivor path memory (SPM) 61, as shown for example in Figure 4, is implemented by using the register-exchange method, as for example described in the patent application GB-A-2286952, published on 30 August 1995.

The branch metric (BM) units in a conventional MLSD (Viterbi) detector require only signal sample inputs, obtained directly from the equalizer (signal labeled B in Figure 2C). As indicated in Figure 4, it is a distinguished feature of the NPML detectors with $K < L$ that each BM unit 62, 63 requires signal samples processed by a predictor 41 (signal labeled z_n in Figure 2C), as well as an additional input from FIR or RAM-based filters 64, 65 (signals Gs_i and Gs_j in Figure 4) in the feedback path between the SPM 61 and the MUU 68. Note that the feedback filters 64, 65 do not have a common serial input, but they are loaded in parallel at every symbol interval T. The input of each FIR

or RAM-based filter 64, 65 is a set of most recent past decisions taken from the survivor path history stored in the SPM 61 for each hypothesized state (i.e., s_i and s_j, respectively, in Figure 4). The add-compare-select (ACS) unit 66 in Figure 3 adds the branch metrics to the state metrics Ms_i and Ms_j, respectively, compares the results, selects the survivor metric Ms_k and provides the update signal Ss_k for the corresponding decision path in the SPM 61. The SPM 61 produces final decisions at output line 67 with a delay of dT seconds relative to time nT. It is a further feature of the present NPML detector that the delay parameter d can generally be made shorter compared to that of a conventional MLSD detector designed for PR signaling (i.e., PR signaling schemes with spectral nulls, such as PR4).

NPML Detector Using Four Predictor Coefficients (N=4) and Two States (K=1):

For N=4 and K=1 the branch metrics based on (5) become

$$\lambda(s_j, s_k) = \left| z_n + \sum_{i=2}^{6} a_{n-i}(s_j) g_i + a_{n-1} g_1 - a_n \right|^2 \qquad (7)$$

where the signal sample $z_n = y_n - \sum_{i=1}^{4} y_n$ .p. is the output of the prediction error filter 41. Associating the data symbols "+1" and "-1" with the binary numbers 1 and 0, respectively, the state information $a_{n-1} = +1(-1)$ is mapped into the present state $s_i = 1(0)$ and the present data symbol $a_n = +1(-1)$ mapped into the next state $s_k = 1(0)$. Letting

$$G1_{n-1} = \sum_{i=2}^{6} a_{n-i}(1) g_i \quad . \qquad (8)$$

$$G0_{n-1} = \sum_{i=2}^{6} a_{n-i}(0)g_i \quad . \tag{9}$$

one obtains the four branch metrics

$$\lambda(1,1) = |z_n + G1_{n-1} + g_1 - 1|^2 \quad . \tag{10}$$

$$\lambda(1,0) = |z_n + G1_{n-1} + g_1 + 1|^2 \quad . \tag{11}$$

$$\lambda(0,1) = |z_n + G0_{n-1} - g_1 - 1|^2 \quad . \tag{12}$$

$$\lambda(0,0) = |z_n + G0_{n-1} - g_1 + 1|^2 \quad . \tag{13}$$

where z_n are the samples obtained from the corresponding 4-tap prediction error filter connected in cascade with the equalizer (see Figure 2C). It will be useful to define the quantities

tp1958v285X

$$Z11_n = z_n + g_1 - 1 \quad . \tag{14}$$

$$Z10_n = z_n + g_1 + 1 \quad . \tag{15}$$

$$Z01_n = z_n - g_1 - 1 \quad . \tag{16}$$

$$Z00_n = z_n - g_1 + 1 \quad . \tag{17}$$

since they can be precomputed outside the feedback loop, if necessary by means of pipelining. Thus, eqs. (10) - (13) can be written as

$$\lambda(1,1) = |Z11_n - G1_{n-1}|^2 . \quad (18)$$

$$\lambda(1,0) = |Z10_n + G1_{n-1}|^2 , \quad (19)$$

$$\lambda(0,1) = |Z01_n + G0_{n-1}|^2 , \quad (20)$$

$$\lambda(0,0) = |Z00_n + G0_{n-1}|^2 . \quad (21)$$

respectively. Finally, defining the stored metrics $M1_n$ and $M0_n$ for states 1 and 0, respectively, the trellis diagram shown in Figure 5 is obtained. The metrics are updated according to

$$M1_n = \min\{M1_{n-1} + \lambda(1,1);\ M0_{n-1} + \lambda(0,1)\} , \quad (22)$$

$$M0_n = \min\{M1_{n-1} + \lambda(1,0);\ M0_{n-1} + \lambda(0,0)\} . \quad (23)$$

and direct mapping of the trellis shown in Figure 5 into hardware functions leads to the implementation of the 2-state NPML detector with a 4-tap predictor 77 shown in Figure 6. It is proposed here to generate the terms $G1_{n-1}$ and $G0_{n-1}$, defined by (8) and (9), respectively, by means of RAM-based filter structures 71, 72 which can be loaded with the appropriate (five) path history decisions. Also indicated in Figure 6 is the 2-state SPM 70 fed by the two comperators 58. In an alternate embodiment (not shown), the functions of SPM 70 and RAM-based filters 71, 72 shown in Figure 6 could be combined in an attempt to speed-up computation of $G1_{n-1}$ and $G0_{n-1}$. Note further, that the squaring functions in Figure 6, realized by means of units 73-76, can be approximated to simplify the required circuitry, with minimal loss in performance. The decision signals S1 and S0 in Figure 6 are used to control

the metric multiplexers 79 and the path update in the SPM 70. The selected metrics $M1_n$ and $M0_n$ are stored in registers 80 and 81, respectively.

A multitude of variations of the implementation shown in Figure 6 is possible, depending on constraints, complexity, critical timing paths, and algorithmic issues such as metric bounding. For example, automatic metric bounding can be achieved by using the conventional modulo technique in the adders 82-85 feeding the comparator inputs 58, as described in "An Alternative to metric rescaling in Viterbi decoders," A.P. Hekstra, IEEE Transactions on Communications, Vol. 37, No. 11, pp. 1220 -1222, November 1989. An alternate method of metric normalization can be implemented by applying the concept of a difference metric. Defining the difference metric

$$D_{n-1} = M1_{n-1} - M0_{n-1} \tag{24}$$

the trellis in Figure 7 is obtained where the metrics are updated such that the metric for state 0 is always the zero-valued metric. Thus, the difference metric is updated according to

$$D_n = \min\{D_{n-1} + \lambda(1,1);\ \lambda(0,1)\} - \min\{D_{n-1} + \lambda(1,0);\ \lambda(0,0)\} \tag{25}$$

where one can show that the cross-extension of the trellis in Figure 7, which would lead to the difference metric $D_n = \lambda(0,1) - [D_{n-1} + \lambda(1,0)]$, is *not* possible. Thus, only three of the four potential values of D_n in (25) will have to be considered. One possible way of mapping the algorithm implied by the trellis description in Figure 7 into hardware is shown in Figure 8 where the threshold for the comparators is now provided by the difference metric D_{n-1} stored in register 80. Figure 8 is otherwise similar to Figure 6. The difference metric approach is useful in cases where it is not possible or convenient to use the conventional modulo technique which relies on 2s-complement arithmetic for metric normalization.

NPML Detector Using Two Predictor Coefficients (N = 2) and Four States (K = 2):

For N=2 and K=2, i.e., $2^K = 4$ states, the branch metrics based on (5) become

$$\lambda(s_j, s_k) = \left| z_n + \sum_{i=3}^{4} a_{n-i}(s_j)g_i + a_{n-1}g_1 + a_{n-2}g_2 - a_n \right|^2 \qquad (26)$$

where the signal sample $z_n = y_n - y_{n-1}p_1 - y_{n-2}p_2$ is the output of the 2-tap prediction error filter. Associating again the data symbols "+1" and "-1" with the binary numbers 1 and 0, respectively, we map the state information $(a_{n-2}, a_{n-1}) = (-1,-1),(-1,+1),(+1,-1)$ and $(+1,+1)$ into the present state $s_j = 0, 1, 2,$ and 3, respectively. Similarly, the next state information $(a_{n-1}, a_n) = (-1,-1),(-1,+1),(+1,-1)$ and $(+1,+1)$ is mapped into the next state $s_k = 0, 1, 2,$ and 3, respectively. Letting

$$G3_{n-1} = \sum_{i=3}^{4} a_{n-i}(3)g_i = a_{n-3}(3)g_3 + a_{n-4}(3)g_4 \,. \qquad (27)$$

$$G2_{n-1} = \sum_{i=3}^{4} a_{n-i}(2)g_i = a_{n-3}(2)g_3 + a_{n-4}(2)g_4 \,. \qquad (28)$$

$$G1_{n-1} = \sum_{i=3}^{4} a_{n-i}(1)g_i = a_{n-3}(1)g_3 + a_{n-4}(1)g_4 \,. \qquad (29)$$

$$G0_{n-1} = \sum_{i=3}^{4} a_{n-i}(0)g_i = a_{n-3}(0)g_3 + a_{n-4}(0)g_4 \,. \qquad (30)$$

one obtains the eight branch metrics

$$\lambda(3,3) = | z_n + G3_{n-1} + g_1 + g_2 - 1 |^2 . \quad (31)$$

$$\lambda(3,2) = | z_n + G3_{n-1} + g_1 + g_2 + 1 |^2 . \quad (32)$$

$$\lambda(2,1) = | z_n + G2_{n-1} + g_1 - g_2 - 1 |^2 . \quad (33)$$

$$\lambda(2,0) = | z_n + G2_{n-1} + g_1 - g_2 + 1 |^2 . \quad (34)$$

$$\lambda(1,3) = | z_n + G1_{n-1} - g_1 + g_2 - 1 |^2 . \quad (35)$$

$$\lambda(1,2) = | z_n + G1_{n-1} - g_1 + g_2 + 1 |^2 . \quad (36)$$

$$\lambda(0,1) = | z_n + G0_{n-1} - g_1 - g_2 - 1 |^2 . \quad (37)$$

$$\lambda(0,0) = | z_n + G0_{n-1} - g_1 - g_2 + 1 |^2 . \quad (38)$$

where z_n are the samples obtained from the corresponding 2-tap predictor filter connected in cascade with the equalizer, see Figure 2C. It will be useful to define the quantities

$$Z33_n = z_n + g_1 + g_2 - 1 . \quad (39)$$

$$Z32_n = z_n + g_1 + g_2 + 1 . \quad (40)$$

$$Z21_n = z_n + g_1 - g_2 - 1 \quad . \tag{41}$$

$$Z20_n = z_n + g_1 - g_2 + 1 \quad . \tag{42}$$

$$Z13_n = z_n - g_1 + g_2 - 1 \quad . \tag{43}$$

$$Z12_n = z_n - g_1 + g_2 + 1 \quad . \tag{44}$$

$$Z01_n = z_n - g_1 - g_2 - 1 \quad . \tag{45}$$

$$Z00_n = z_n - g_1 - g_2 + 1 \quad . \tag{46}$$

since they can be precomputed outside the feedback loop, if necessary by means of pipelining. Thus, eqs. (31) - (38) can be written as

$$\lambda(3,3) = |Z33_n - G3_{n-1}|^2 \quad . \tag{47}$$

$$\lambda(3,2) = |Z32_n - G3_{n-1}|^2 \quad . \tag{48}$$

$$\lambda(2,1) = |Z21_n - G2_{n-1}|^2 \quad . \tag{49}$$

$$\lambda(2,0) = |Z20_n - G2_{n-1}|^2 \quad . \tag{50}$$

$$\lambda(1,3) = |Z13_n - G1_{n-1}|^2 \quad . \tag{51}$$

$$\lambda(1,2) = |Z12_n + G1_{n-1}|^2 . \quad (52)$$

$$\lambda(0,1) = |Z01_n + G0_{n-1}|^2 . \quad (53)$$

$$\lambda(0,0) = |Z00_n + G0_{n-1}|^2 . \quad (54)$$

respectively. Finally, defining the stored (present) metrics $Ms_{i_{n-1}}$ for each of the present states $s_i = 0,1,2$, and 3, one obtains the trellis diagram shown in Figure 9. The four metrics for the next states $s_i = 0,1,2$, and 3, are updated according to

$$Ms_{k_n} = \min \{Ms_{j_{n-1}} + \lambda(s_j, s_k);\ Ms_{i_{n-1}} + \lambda(s_i, s_k)\} , \quad (55)$$

with s_j and s_i being the possible present states. Direct mapping of the trellis shown in Figure 9 into hardware functions leads to the scheme shown in Figures 10A, 10B, 10C. The terms $G0_{n-1}$, $G1_{n-1}$, $G2_{n-1}$, and $G3_{n-1}$, defined by (27) - (30), respectively, can be generated by means of a random access memory 131-134 (RAM) which stores the appropriate values for the given coefficient g_1 and g_2, depending on the chosen operating point of the channel; the RAMs 131-134 need to hold only four different (actually two different and their negative) values. The 4-state SPM 135 is a register-exchange structure in case of high-speed implementation. Note that the squaring functions in (31) - (38) can be approximated to simplify the required circuitry, with minimal loss in performance. Four decision signals (S0, S1, S2, S3) are needed to control the metric multiplexers and the path update in the SPM 135. Automatic metric bounding is achieved by using the conventional modulo-2 technique in the adders 136-143 feeding the comparator inputs.

NPML Detector Using Four Predictor Coefficients (N=4) and Four States (K=2):

For N=4 and K=2, i.e., $2^K = 4$ states, the branch metrics based on (5) become

$$\lambda(s_j, s_k) = \left| z_n + \sum_{i=3}^{6} a_{n-i}(s_j)g_i + a_{n-1}g_1 - a_{n-2}g_2 - a_n \right|^2 \qquad (56)$$

where the signal sample $z_n = y_n - \sum_{i=1}^{4} y_{n-i}p_i$ is the output of the prediction error filter. Associating again the data symbols "+1" and "-1" with the binary numbers 1 and 0, respectively, the state information $(a_{n-2}, a_{n-1}) = (-1,-1),(-1,+1),(+1,-1)$, and $(+1,+1)$, is mapped into the present state $s_j = 0, 1, 2$, and 3, respectively. Similarly, the next state information $(a_{n-1}, a_n) = (-1,-1),(-1,+1),(+1,-1)$, and $(+1,+1)$, is mapped into the next state $s_k = 0, 1, 2$, and 3, respectively. Letting

$$G3_{n-1} = \sum_{i=3}^{6} a_{n-i}(3)g_i \; . \qquad (57)$$

$$G2_{n-1} = \sum_{i=3}^{6} a_{n-i}(2)g_i \; . \qquad (58)$$

$$G1_{n-1} = \sum_{i=3}^{6} a_{n-i}(1)g_i \; . \qquad (59)$$

$$G0_{n-1} = \sum_{i=3}^{6} a_{n-i}(0)g_i \; . \qquad (60)$$

one obtains the eight branch metrics

$$\lambda(3,3) = |z_n + G3_{n-1} + g_1 + g_2 - 1|^2 . \quad (61)$$

$$\lambda(3,2) = |z_n + G3_{n-1} + g_1 + g_2 + 1|^2 . \quad (62)$$

$$\lambda(2,1) = |z_n + G2_{n-1} + g_1 - g_2 - 1|^2 . \quad (63)$$

$$\lambda(2,0) = |z_n + G2_{n-1} + g_1 - g_2 + 1|^2 . \quad (64)$$

$$\lambda(1,3) = |z_n + G1_{n-1} - g_1 + g_2 - 1|^2 . \quad (65)$$

$$\lambda(1,2) = |z_n + G1_{n-1} - g_1 + g_2 + 1|^2 . \quad (66)$$

$$\lambda(0,1) = |z_n + G0_{n-1} - g_1 - g_2 - 1|^2 . \quad (67)$$

$$\lambda(0,0) = |z_n + G0_{n-1} - g_1 - g_2 + 1|^2 . \quad (68)$$

where z_n are the samples obtained from the corresponding 4-tap prediction error filter connected in cascade with the equalizer (see Figure 2C). It is useful to define the quantities

$$Z33_n = z_n + g_1 + g_2 - 1 . \quad (69)$$

$$Z32_n = z_n + g_1 + g_2 + 1 . \quad (70)$$

$$Z21_n = z_n + g_1 - g_2 - 1 \quad . \tag{71}$$

$$Z20_n = z_n + g_1 - g_2 + 1 \quad . \tag{72}$$

$$Z13_n = z_n - g_1 - g_2 - 1 \quad . \tag{73}$$

$$Z12_n = z_n - g_1 + g_2 + 1 \quad . \tag{74}$$

$$Z01_n = z_n - g_1 - g_2 - 1 \quad . \tag{75}$$

$$Z00_n = z_n - g_1 - g_2 + 1 \quad . \tag{76}$$

since they can be precomputed outside the feedback loop, if necessary by means of pipelining. Thus, eqs. (61) - (68) can be written as

$$\lambda(3,3) = |Z33_n + G3_{n-1}|^2 \quad . \tag{77}$$

$$\lambda(3,2) = |Z32_n + G3_{n-1}|^2 \quad . \tag{78}$$

$$\lambda(2,1) = |Z21_n + G2_{n-1}|^2 \quad . \tag{79}$$

$$\lambda(2,0) = |Z20_n + G2_{n-1}|^2 \quad . \tag{80}$$

$$\lambda(1,3) = |Z13_n + G1_{n-1}|^2 \quad . \tag{81}$$

$$\lambda(1,2) = |Z12_n + G1_{n-1}|^2 , \quad (82)$$

$$\lambda(0,1) = |Z01_n + G0_{n-1}|^2 , \quad (83)$$

$$\lambda(0,0) = |Z00_n + G0_{n-1}|^2 , \quad (84)$$

respectively. Finally, defining the stored (present) metrics $Ms_{i_{n-1}}$ for each of the present states $s_i = 0, 1, 2,$ and 3, one obtains the trellis diagram shown in Figure 9. The four metrics for the next states $s_k = 0, 1, 2,$ and 3, are updated according to

$$Ms_{k_n} = \min \{Ms_{j_{n-1}} + \lambda(s_j, s_k);\ Ms_{i_{n-1}} + \lambda(s_i, s_k)\} , \quad (85)$$

with s_j and s_i being the possible present states. Direct mapping of the trellis shown in Figure 9 into hardware functions leads to an implementation structure shown in Figures 11A, 11B, and 11C. Note the similarity, respectively the differences, compared to Figures 10A, 10B, 10C (size of predictor filter and RAM address length). The terms $G0_{n-1}$, $G1_{n-1}$, $G2_{n-1}$, and $G3_{n-1}$, defined by (57) - (60), respectively, can be generated by means of RAM structures which can be loaded with appropriate values depending on the chosen operating point of the channel; the 4-state SPM can again be a register-exchange structure. Note that the squaring functions in (61) - (68) can be approximated to simplify the required circuitry, with minimal loss in performance. Four decision signals S0, S1, S2, and S3, are needed to control the metric multiplexers and the path update in the SPM.

A multitude of variations for the implementation of the 4-state NPML detector with a 4-tap noise predictor is possible, depending on constraints on complexity, critical timing paths, and algorithmic issues such as metric bounding. For example, automatic metric bounding can be achieved by using

the conventional modulo technique in the adders feeding the comparator inputs. The alternate method of metric normalization, the difference metric technique introduced above, can be extended to the 4-state NPML detector, for example, by updating the metrics such that the stored metric of state 0 is always the zero-valued metric. Further variations for implementing (4-state) NPML detectors can be obtained by explicit expansion of the squaring function involved in evaluating the branch metrics $\lambda(s_j, s_k)$.

NPML Detector Using a Single-Tap Predictor (N=1) and Eight States (K=N+2=3):

It was pointed out hereinbefore that the 8-state NPML detector which uses a single-tap predictor (i.e., the case where N=1 and K=N+2=3 so that $2^K = 8$ states) is a member within the family of NPML detectors which is of specific practical interest for DASD applications. Since in this particular case there is no feedback based on past decisions, i.e., the detector uses only (hypothesized) state information for noise prediction, the feedback loops via the FIR or RAM-based filters 64 and 65, as shown in Figure 4, are not present. For N=1 and K=3 the 16 branch metrics based on (5) become

$$\lambda(s_j, s_k) = | z_n + a_{n-1}g_1 + a_{n-2}g_2 + a_{n-3}g_3 - a_n |^2 \qquad (86)$$

where the signal sample $z_n = y_n - p_1 y_{n-1}$. Furthermore, since in (86) $g_1 = p_1$, $g_2 = 1$, and $g_3 = -p_1$, we can write

$$\lambda(s_j, s_k) = | z_n + a_{n-1}p_1 + a_{n-2} - a_{n-3}p_1 - a_n |^2 \qquad (87)$$

where the triple $(a_{n-3}, a_{n-2}, a_{n-1})$ represents the hypothesized state s_j, a_n is the hypothesized transmitted symbol, and the triple (a_{n-2}, a_{n-1}, a_n) represents the resulting next state s_k. In this situation it is advantageous to evaluate the square on the right hand side of (87), to drop all state-independent terms, and

to scale the remaining expression. In this way, one arrives at the equivalent branch metric

$$\begin{aligned}\lambda'(s_j, s_k) = &-[a_n - a_{n-2} - (a_{n-1} - a_{n-3})p_1]z_n \\ &- (a_n a_{n-1} + a_{n-2}a_{n-3})p_1 - a_n a_{n-2} \\ &+ (a_n a_{n-3} + a_{n-1}a_{n-2})p_1 - a_{n-1}a_{n-3}p_1^2 .\end{aligned} \tag{88}$$

We now arbitrarily use a somewhat different rule than the one used above to map the state information into the corresponding state number, namely, $s_j = (a_{n-3}, a_{n-2}, a_{n-1}) = (-1, -1, -1)$ maps to the state 0, $s_j = (a_{n-3}, a_{n-2}, a_{n-1}) = (+1, -1, -1)$ maps to the state 1, ..., $s_j = (a_{n-3}, a_{n-2}, a_{n-1}) = (+1, +1, +1)$ maps to state 7. Next, adding the state-independent term $(1 + p_1^2)$ to all sixteen branch metrics represented by (88) and dividing the result by 2, the equivalent branch metrics can be listed as

$$\lambda''(0,0) = \lambda''(2,5) = \lambda''(5,2) = \lambda''(7,7) = 0 \tag{89}$$

$$\lambda''(0,4) = \lambda''(5,6) = -z_n + 1 \tag{90}$$

$$\lambda''(1,0) = \lambda''(3,5) = p_1(-z_n + p_1) \tag{91}$$

$$\lambda''(1,4) = \alpha(-z_n + \alpha) \tag{92}$$

$$\lambda''(2,1) = \lambda''(7,3) = z_n + 1 \tag{93}$$

$$\lambda''(3,1) = \beta(z_n + \beta) \tag{94}$$

$$\lambda''(4,2) = \lambda''(6,7) = p_1(z_n + p_1) \tag{95}$$

$$\lambda''(4,6) = \beta(-z_n + \beta) \tag{96}$$

$$\lambda''(6,3) = \alpha(z_n + \alpha) \tag{97}$$

where

$$\alpha = 1 + p_1,\ \beta = 2 - \alpha = 1 - p_1,\ z_n = y_n - p_1 y_{n-1}\ . \tag{98}$$

Defining the stored metrics Ms_{j_n} for the states $s_j = 0, 1, \ldots, 7$, one arrives at the trellis diagram shown in Figure 12. The eight metrics Ms_{k_n} for the next states $s_k = 0, 1, \ldots, 7$, are updated according to

$$Ms_{k_n} = \min\{Ms_{j_{n-1}} + \lambda''(s_j, s_k);\ Ms_{i_{n-1}} + \lambda''(s_i, s_k)\}\ , \tag{99}$$

with s_j and s_i being the states at time n-1, according to the trellis in Figure 12. The latter can in principle be mapped directly into a hardware structure.

The trellis in Figure 12 can be further simplified by applying a similar transformation technique as described in the patent application GB-A-2286952, published on 30 August 1995; the resulting transformed trellis is shown in Figure 13 where 12 of the 16 branch metrics are zero-valued and the remaining four have values $2p_1$ or $-2p_1$. Defining the filtered samples

$$Y_n = -p_1 y_{n+1} + (1 + p_1^2) y_n - p_1 y_{n-1} \tag{100}$$

where $y_n = a_n - a_{n-2} +$ noise is the PR4-equalized, noisy sample, the quantities Z_n and Q_n shown in the trellis of Figure 13 can be expressed as

$$Z_n = Y_n + (1 + p_1^2) \tag{101}$$

and

$$Q_n = -Y_n + (1 + p_1^2) = -Z_n + 2(1 + p_1^2) \ . \tag{102}$$

respectively: if necessary, these quantities can be computed by pipelined circuitry since they are not part of the metric feedback loop. Direct mapping of the trellis in Figure 13 into a hardware structure leads to the scheme shown in Figure 14: the eight decision signals S0 - S7 also control the operation of an 8-state SPM (register-exchange) not specifically shown. The SPM delivers the final decisions via the inverse precoder.

A significant feature of the NPML scheme described by Figures 12 - 14 is its ability to perform the detection function for arbitrary values of the noise predictor coefficient p_1. Thus, by programming the hardware with the best suited predictor coefficient (depending on the channel operating point), optimal detection is obtained within the constraints of a single-tap predictor. In particular, by setting $p_1 = 0$, the scheme performs detection for PR4 signals, i.e., the hardware operates as a PRML detector. On the other hand, setting $p_1 = -1$, the scheme performs detection for EPR4 signals, i.e., the hardware operates as an EPRML detector. The maximum required length of the SPM or, equivalently, the maximum decision delay for the final decisions, should be chosen such that the performance can be maintained for the most sensitive scheme (e.g. EPRML).

For implementation purposes, it may be advantageous to modify the algorithm outlined for the flexible 8-state, single-tap predictor NPML scheme by adding a convenient, state-independent term to Z_n defined in eq. (101), e.g., such that $Z_n \rightarrow Z'_n = Y_n$. It has been shown in the patent application GB-A-2286952, published on 30 August 1995, that the performance of the EPRML is not affected by such a measure since the channel is DC-free (spectral null at zero

frequency); this property extends to NPML detectors as well. Thus, an alternate version of the scheme in Figure 14 is obtained by modifying Z_n and Q_n such that $Z_n \rightarrow Z'_n = Y_n$ and $Q_n \rightarrow Q'_n = -Y_n + 2(1 + p_1^2) = -Z'_n + 2(1 + p_1^2)$, respectively. Note that the condition $Z_n + Q_n = Z'_n + Q'_n = 2(1 + p_1^2)$, must always be satisfied by theory. However, as described in the patent application GB-A-2286952, published on 30 August 1995, it may be advantageous in practice to modify this condition such that $Z_n + Q_n = Z'_n + Q'_n = 2(1 + p_1^2) - \gamma$, where γ is a small, positive constant; a practical value may be $\gamma = 0.25$.

Alternate Forms of Implementation and Modifications:

This section further demonstrates the multitude of forms of implementation which are possible for NPML detectors according to the present invention. Some alternate forms and simplifications of the detectors presented above are now described in some detail:

2-State, 4-Tap Predictor NPML:

Letting

$$G1'_{n-1} = g_1 + \sum_{i=2}^{6} a_{n-i}(1)g_i \quad . \tag{103}$$

$$G0'_{n-1} = -g_1 + \sum_{i=2}^{6} a_{n-i}(0)g_i \quad . \tag{104}$$

one obtains the four equivalent branch metrics

$$\lambda(1,1) = |z_n + G1'_{n-1} - 1|^2 \quad . \tag{105}$$

$$\lambda(1,0) = |z_n + G1'_{n-1} + 1|^2 . \quad (106)$$

$$\lambda(0,1) = |z_n + G0'_{n-1} - 1|^2 . \quad (107)$$

$$\lambda(0,0) = |z_n + G0'_{n-1} + 1|^2 . \quad (108)$$

where z_n are the samples obtained from the corresponding 4-tap prediction error filter connected in cascade with the equalizer (see Figure 2C). It is useful to define the new quantities

$$Z1_n = z_n - 1 . \quad (109)$$

$$Z0_n = z_n + 1 . \quad (110)$$

so that eqs. (105) - (108) can be written as

$$\lambda(1,1) = |Z1_n + G1'_{n-1}|^2 . \quad (111)$$

$$\lambda(1,0) = |Z0_n + G1'_{n-1}|^2 . \quad (112)$$

$$\lambda(0,1) = |Z1_n + G0'_{n-1}|^2 . \quad (113)$$

$$\lambda(0,0) = |Z0_n + G0'_{n-1}|^2 . \quad (114)$$

The alternate form of implementing the functions of Figure 6 is shown in Figure 15. Here, it is proposed to generate the terms $G1'_{n-1}$ and $G0'_{n-1}$, defined by (103) and (104), respectively, by means of random access memory

table look-up where the RAMs 121, 122 can be loaded with appropriate values (32 for each RAM) depending on the chosen operating point of the channel. The SPM 123 provides the five address bits $a_{n-2}(1), \ldots, a_{n-6}(1)$ and $a_{n-2}(0), \ldots, a_{n-6}(0)$ for the RAMs 121 and 122, respectively, as indicated in Figure 15.

Computation of the branch metrics for the difference metric approach (Figure 8) can be modified similarly; in this case, further simplifications are possible. For example, the potential difference metrics $D_n = \lambda(0,1) - \lambda(0,0) = -4(z_n + G0'_{n-1})$ and $D_n = \lambda(1,1) - \lambda(1,0) = -4(z_n + G1'_{n-1})$ which have to be precomputed, have simple expressions in terms of the signal sample z_n and the respective quantities generated by the RAMs.

4-State, N-Tap Predictor NPML where N=2 or 4 (Alternative 1):

Letting

$$G3'_{n-1} = g_1 + g_2 + \sum_{i=3}^{N+2} a_{n-i}(3)g_i \quad . \tag{115}$$

$$G2'_{n-1} = g_1 - g_2 + \sum_{i=3}^{N+2} a_{n-i}(2)g_i \quad . \tag{116}$$

$$G1'_{n-1} = -g_1 + g_2 + \sum_{i=3}^{N+2} a_{n-i}(1)g_i \quad . \tag{117}$$

$$G0'_{n-1} = -g_1 - g_2 + \sum_{i=3}^{N+2} a_{n-i}(0)g_i \quad . \tag{118}$$

one obtains the eight equivalent branch metrics

$$\lambda(3,3) = |z_n + G3'_{n-1} - 1|^2 . \quad (119)$$

$$\lambda(3,2) = |z_n + G3'_{n-1} + 1|^2 . \quad (120)$$

$$\lambda(2,1) = |z_n + G2'_{n-1} - 1|^2 . \quad (121)$$

$$\lambda(2,0) = |z_n + G2'_{n-1} + 1|^2 . \quad (122)$$

$$\lambda(1,3) = |z_n + G1'_{n-1} - 1|^2 . \quad (123)$$

$$\lambda(1,2) = |z_n + G1'_{n-1} + 1|^2 . \quad (124)$$

$$\lambda(0,1) = |z_n + G0'_{n-1} - 1|^2 . \quad (125)$$

$$\lambda(0,0) = |z_n + G0'_{n-1} + 1|^2 . \quad (126)$$

where z_n are the samples obtained from the corresponding N-tap prediction error filter connected in cascade with the equalizer (see Figure 2C). By making use of the definitions $Z1_n = z_n - 1$ and $Z0_n = z_n + 1$, respectively, eqs. (119) - (126) can be written as

$$\lambda(3,3) = |Z1_n + G3'_{n-1}|^2 . \quad (127)$$

$$\lambda(3,2) = |Z0_n + G3'_{n-1}|^2 . \quad (128)$$

$$\lambda(2,1) = |Z1_n + G2'_{n-1}|^2 . \quad (129)$$

$$\lambda(2,0) = |Z0_n + G2'_{n-1}|^2 . \quad (130)$$

$$\lambda(1,3) = |Z1_n + G1'_{n-1}|^2 . \quad (131)$$

$$\lambda(1,2) = |Z0_n + G1'_{n-1}|^2 . \quad (132)$$

$$\lambda(0,1) = |Z1_n + G0'_{n-1}|^2 . \quad (133)$$

$$\lambda(0,0) = |Z0_n + G0'_{n-1}|^2 . \quad (134)$$

respectively, yielding again the trellis diagram shown in Figure 9. Direct mapping of this trellis into hardware functions - by using the new variables as defined above - leads to the structure shown in Figures 16A, 16B, 16C. The terms $G0'_{n-1}$, $G1'_{n-1}$, $G2'_{n-1}$, and $G3'_{n-1}$, defined by (115) - (118), respectively, can again be generated by means of RAMs 151-154 which can be loaded with the appropriate values depending on the chosen operating point of the channel: the 4-state SPM 155 - assuming again a register-exchange structure - provides the N address bits for each of the four RAMs (one per state); equivalently, these four RAMs 151-154 can be combined into a single RAM structure with multiple inputs and outputs. Automatic metric bounding is achieved by using the conventional modulo-2 technique in the adders feeding the comparator inputs.

NPML Detectors Implemented by Analog VLSI Technology:

Implementation of any detector included within the family of NPML detectors can be done in either digital, analog, or mixed digital/analog VLSI circuit technology. Implementations in analog technology are of particular interest in

high data rate and/or low-power applications. An example for PRML is described in "Analog Implementation of Class-IV Partial-Response Viterbi Detector", A.H. Shakiba et al., Proc. ISCAS'94, 1994; similar methods can be applied to NPML detectors.

NPML Detectors with Reduced SPM Length:

It was indicated above, that NPML detectors generally do not exhibit quasi-catastrophic error propagation. This property can be exploited to save hardware and reduce decoding delay by reducing the length of the path memory in the Viterbi detector without compromising performance. On the other, these hardware savings may be traded for additional increases in recording density by using run-length limited (RLL) codes with a higher rate than 8/9, since the code constraints relating to the length of the SPM can be relaxed.

4-State, N-Tap Predictor NPML where N=2 or 4 (Alternative 2):

Letting in (119) - (126)

$$G33'_{n-1} = G3'_{n-1} - 1 \tag{135}$$

$$G32'_{n-1} = G3'_{n-1} + 1 \tag{136}$$

and so on, we can write the eight branch metrics as

$$\lambda(3,3) = |z_n + G33'_{n-1}|^2 . \tag{137}$$

$$\lambda(3,2) = |z_n + G32'_{n-1}|^2 . \tag{138}$$

$$\lambda(2,1) = |z_n + G21'_{n-1}|^2 . \tag{139}$$

$$\lambda(2,0) = |z_n + G20'_{n-1}|^2 . \quad (140)$$

$$\lambda(1,3) = |z_n + G13'_{n-1}|^2 . \quad (141)$$

$$\lambda(1,2) = |z_n + G12'_{n-1}|^2 . \quad (142)$$

$$\lambda(0,1) = |z_n + G01'_{n-1}|^2 . \quad (143)$$

$$\lambda(0,0) = |z_n + G00'_{n-1}|^2 . \quad (144)$$

This version leads to the implementation shown in Figures 17A, 17B, 17C where the squaring function can be approximated as shown by A. Eshraghi et al., in "Design of a New Squaring Function for the Viterbi Algorithm", IEEE Journal of Solid State Circuits, Vol. 29, No. 9, September 1994, pp. 1102 - 1107.

CLAIMS

THIS SHEET HAS BEEN REPLACED

Amended claim 1

1. Apparatus for noise predictive maximum likelihood (NPML) sequence detection in a channel, comprising:

a) a prediction error filter for whitening colored random noise components of a sample y_n received via said channel, said sample y_n comprising a generalized partial-response signal component corrupted by said colored random noise components, leading to a signal z_n now having L intersymbol-interference components.

b) a sequence detector having

- a state complexity being equal to 2^K, with $0 \leq K \leq L$ and L reflecting the number of said intersymbol interference components, and
- survivor path means for storing path history decisions corresponding to 2^K survivor paths.

c) means for cancellation of L-K of said L intersymbol-interference components, said means comprising

- feedback means for intersymbol-interference cancellation using precomputed and stored intersymbol-interference cancellation terms, and
- means for retrieving said intersymbol-interference cancellation terms by applying said path history decisions as addresses to said feedback means for intersymbol-interference cancellation.

2. The apparatus of claim 1, wherein said means for cancellation comprises at least one random access memory for storing said intersymbol interference cancellation terms, said random access memory being arranged such that intersymbol-interference cancellation terms are retrieved by applying a path history decision taken from said survivor path means as address to said random access memory.

This Sheet Has Been Replaced

3. The apparatus of claim 1, wherein said sample y_n received via said channel is a partial-response signal and in particular a partial-response class-4 (PR4) shaped signal.

4. The apparatus of claim 1, wherein said sequence detector is a Viterbi detector.

5. The apparatus of claim 1, wherein said sequence detector is a 2-state sequence detector and said prediction error filter comprising a 4-tap predictor.

6. The apparatus of claim 1, wherein said sequence detector is a 4-state sequence detector and said prediction error filter comprising a 2-tap predictor.

7. The apparatus of claim 1, wherein said sequence detector is a 4-state sequence detector and said prediction error filter comprising a 4-tap predictor.

8. The apparatus of claim 1, wherein said sequence detector is a 8-state sequence detector, preferably a programmable one, and said prediction error filter comprising a 1-tap predictor.

9. The apparatus of claim 1, either comprising a separate inverse precoder fed by the output of said detector, or means for imbedding the inverse precoder function into said sequence detector.

10. The apparatus of claim 1, having a transfer function for the signal portion of said sample y_n being different from the transfer function for said colored random noise components.

11. The apparatus of claim 2, wherein said prediction error filter and/or said random access memory has a non-linear transfer characteristic.

12. The apparatus of claim 2, wherein said prediction error filter and/or said random access memory is programmable.

13. The apparatus of claim 12, comprising means for adaptive setting of said programmable prediction error filter and/or said random access memory such that its characteristic automatically adjusts as the colored random noise on said data channel changes.

14. The apparatus of claim 1 or 2 being either completely or partially implemented in analog circuit technology.

15. The apparatus of claim 1 or 2, wherein said feedback means comprise a feedback finite-impulse response (FIR) filter.

16. The apparatus of claim 1, comprising:

- a memoryless detector for determining a nominal expected value,
- means for estimating the noise contribution in a plurality of past digital samples by subtracting the value of a sample from said nominal expected value,
- means for predicting the noise contribution of the current received sample using the noise contribution in a plurality of said past digital samples,
- means for adding or subtracting the predicted noise contribution to/from the current received sample, and
- means for feeding the output of the means for adding or subtracting to a conventional partial response maximum likelihood (PRML) or extended partial-response maximum likelihood (EPRML) detector.

17. The apparatus of any of the claims 1-16, wherein said channel is a data transmission channel and said apparatus is employed for estimation of data received via said data transmission channel.

18. Direct access storage device, in particular a disk drive, comprising direct access storage means and an apparatus for noise predictive maximum likelihood (NPML) sequence detection according to any of the claims 1 - 16, said channel being a storage channel for feeding signals retrieved from said direct access storage means to said apparatus.

19. The apparatus of any of the claims 1-16, being integrated into (piggy-backed) on a partial-response maximum likelihood (PRML) or extended partial-response maximum likelihood (EPRML) system.

20. The apparatus of claim 19, wherein a digital equalizer, being part of said partial-response maximum likelihood (PRML) or extended partial-response maximum likelihood (EPRML) system, and said prediction error filter are replaced by a single finite-impulse response filter having the property to whiten said colored random noise components of said sample y_n.

21. The apparatus of any of the claims 1-16, being connected to a partial response maximum likelihood (PRML) or an extended partial-response maximum likelihood (EPRML) detector such that one can switch from a first state where the apparatus and either one of said detectors operate concurrently to a second state where either said partial response maximum likelihood (PRML) or extended partial-response maximum likelihood (EPRML) detector, or said apparatus processes said sample y_n received via said channel.

22. Method for noise predictive maximum likelihood (NPML) sequence detection by means of a sequence detector having a state complexity being equal to 2^K, with $0 \leq K \leq L$, said method comprising the steps:

a) whitening colored random noise components of a sample y_n received via a channel, said sample y_n comprising a generalized partial response signal component corrupted by said colored random noise components, leading to a signal z_n then having L intersymbol-interference components,

b) eliminating K of said L intersymbol-interference components by carrying out a branch metric computation based on a 2^K-State Viterbi algorithm to determine the most likely sequence corresponding to said sample y_n, and

c) if there are any intersymbol-interference components left, i.e., if $L - K > 0$,

- precomputing intersymbol-interference cancellation terms,
- storing said intersymbol-interference cancellation terms in storage means,
- retrieving said intersymbol-interference cancellation terms from said storage means by applying path history decisions from said sequence detector as addresses to said memory means,
- cancelling said L-K intersymbol-interference components in said signal z_n using said intersymbol interference cancellation terms.

23. The method of claim 22, comprising the steps:

- estimating the noise contribution in a plurality of past digital samples by subtracting the value of a sample from a nominal expected value, said nominal expected value being determined by simple memoryless detection,
- using the noise contribution in a plurality of said past digital samples to predict the noise contribution of the current received sample,
- adding or subtracting the predicted noise contribution to/from the current received sample, and
- feeding the output of the last step to a conventional partial response maximum likelihood (PRML) or extended partial-response maximum likelihood (EPRML) detector.

24. The method of claim 22, wherein said sample y_n received via said channel is a partial-response signal and in particular a partial-response class-4 (PR4) shaped signal.

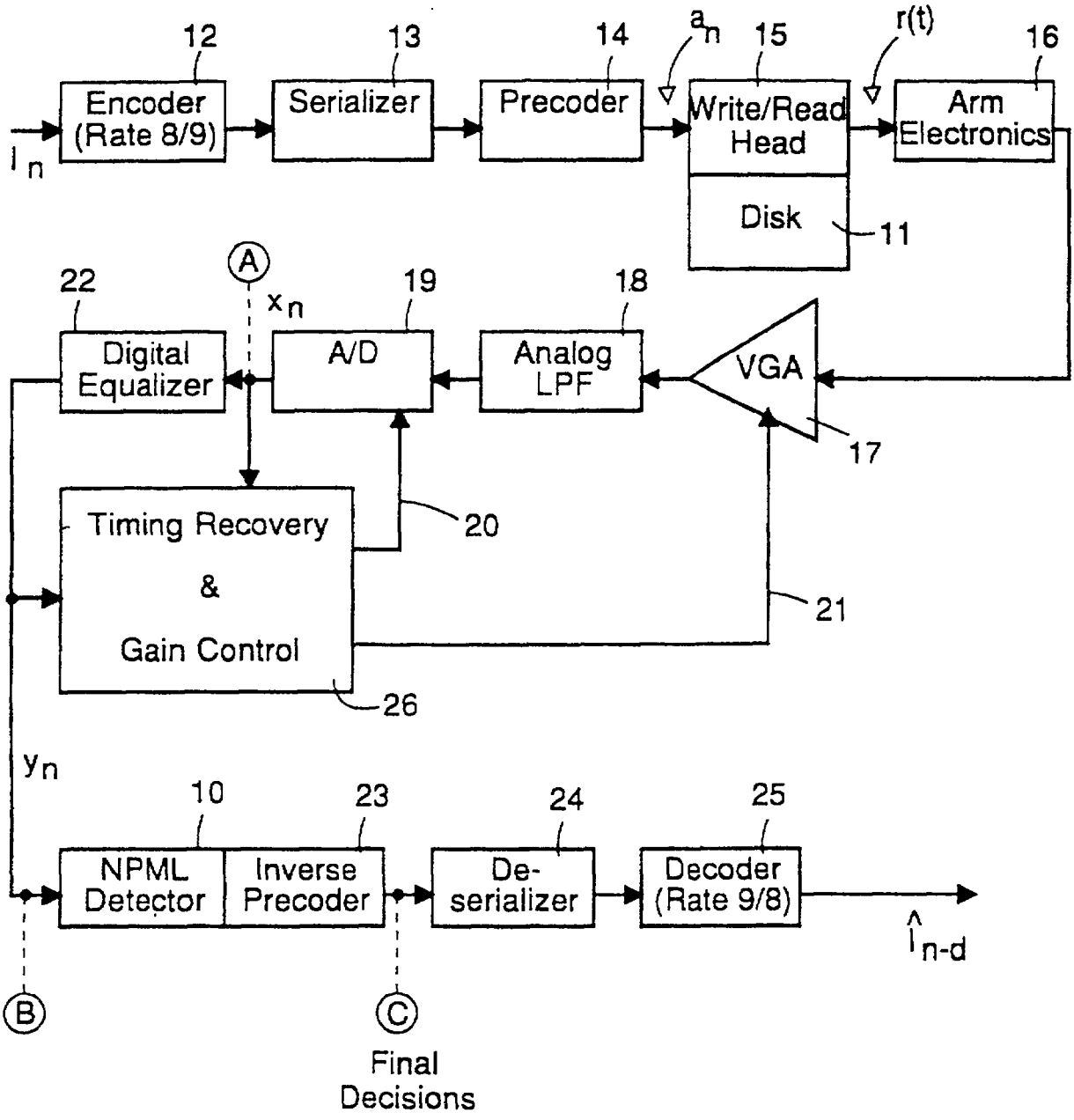

12
13
14
a_n
15
r(t)
16
Encoder (Rate 8/9)
Serializer
Precoder
Write/Read Head
Arm Electronics
I_n
Disk
11
A
x_n
22
19
18
Digital Equalizer
A/D
Analog LPF
VGA
17
Timing Recovery & Gain Control
20
21
26
y_n
10
23
24
25
NPML Detector
Inverse Precoder
De-serializer
Decoder (Rate 9/8)
$\hat{I}_{n-d}$
B
C
Final Decisions

FIG. 1

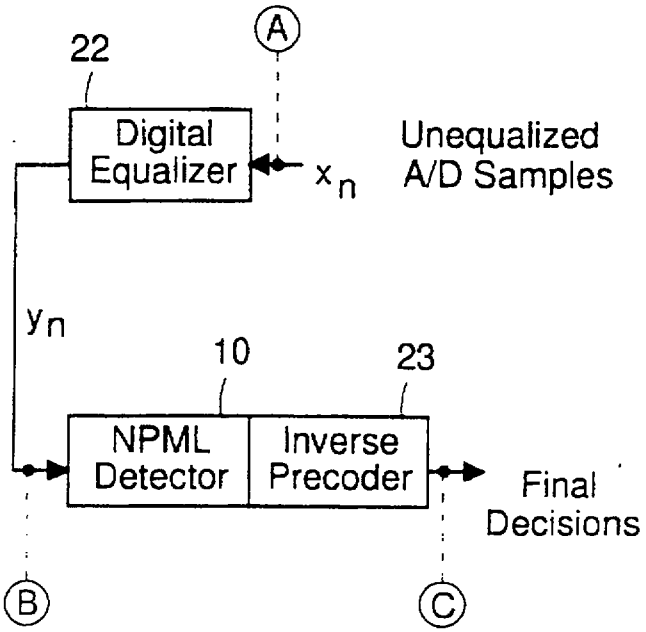

A
22
Digital Equalizer
x_n
Unequalized A/D Samples
y_n
10
23
NPML Detector
Inverse Precoder
Final Decisions
B
C

FIG. 2A

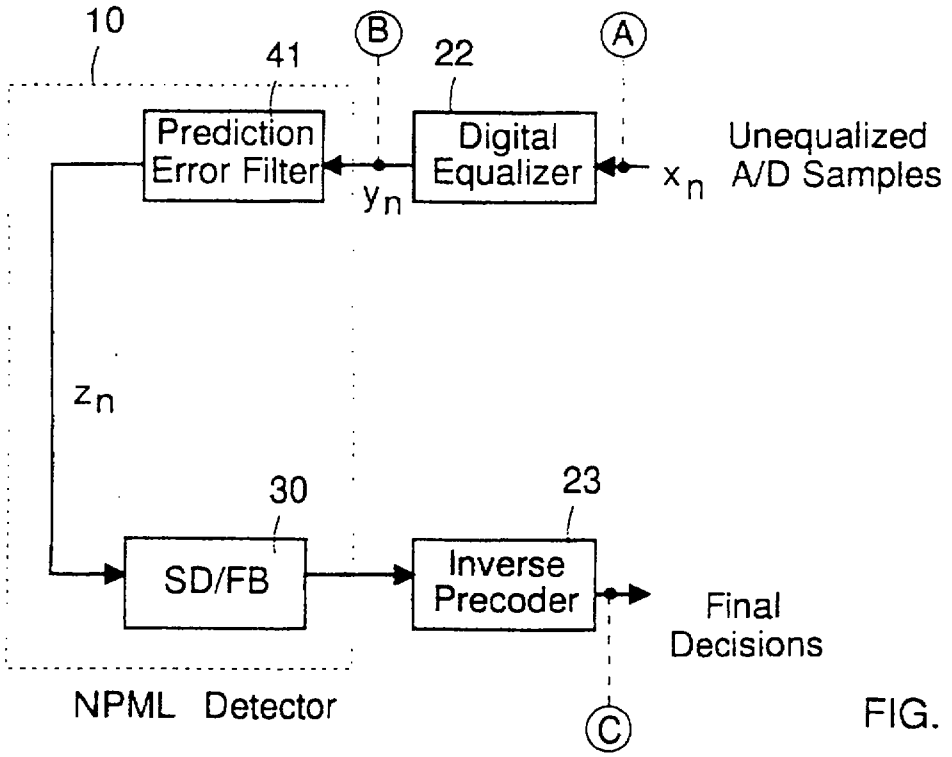

10
B
A
41
22
Prediction Error Filter
Digital Equalizer
x_n
Unequalized A/D Samples
y_n
z_n
30
23
SD/FB
Inverse Precoder
Final Decisions
NPML Detector
C

FIG. 2B

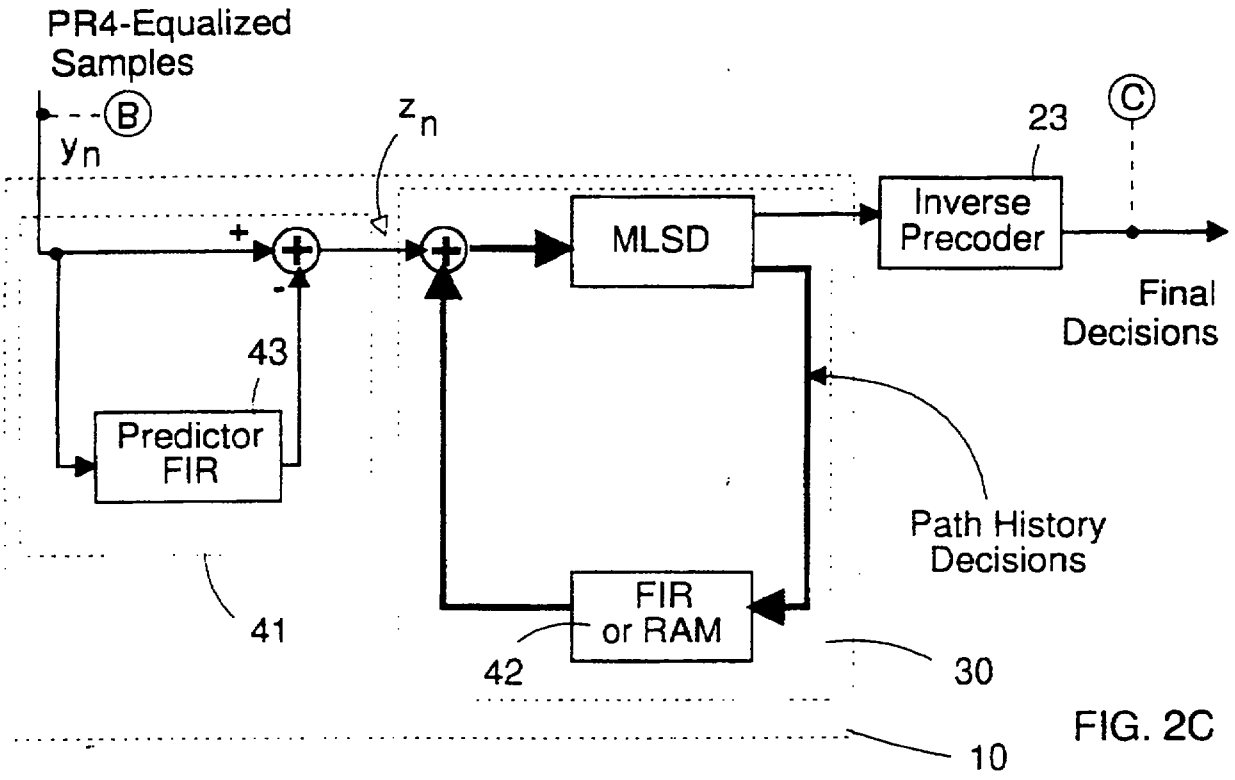

PR4-Equalized Samples
B
yn
zn
23
C
MLSD
Inverse Precoder
Final Decisions
+
-
43
Predictor FIR
Path History Decisions
41
FIR or RAM
42
30
10

FIG. 2C

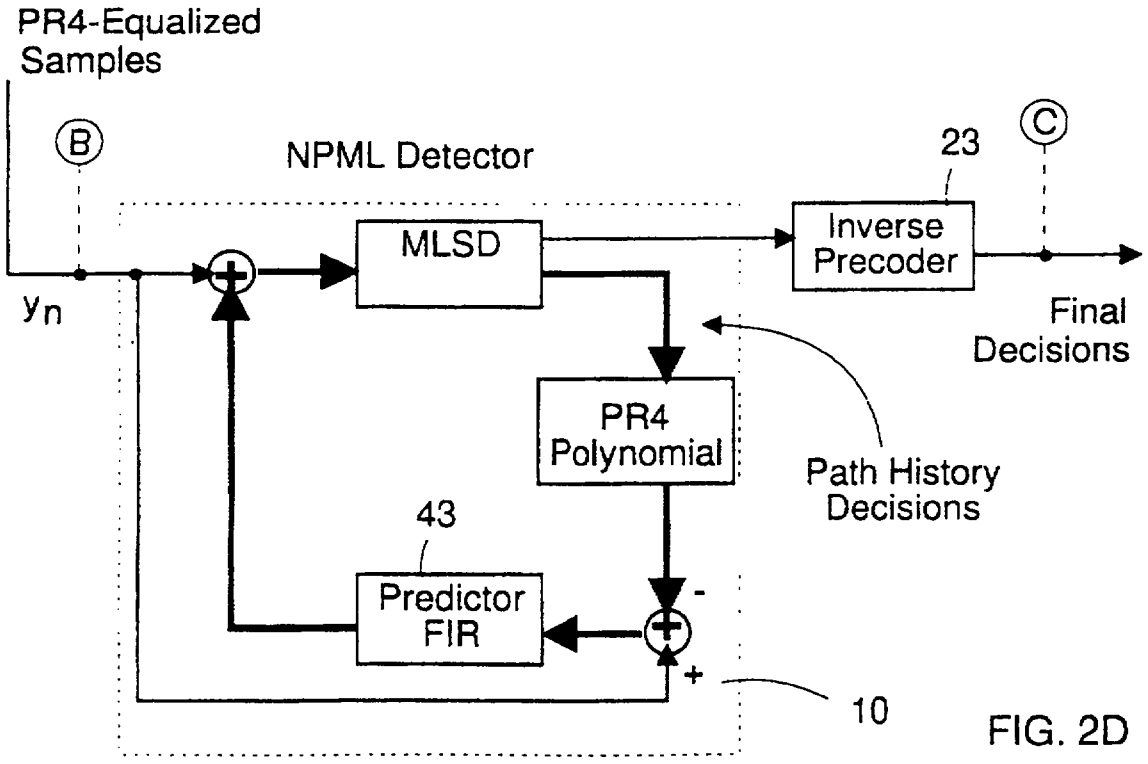

PR4-Equalized Samples
B
NPML Detector
23
C
MLSD
Inverse Precoder
yn
Final Decisions
PR4 Polynomial
Path History Decisions
43
Predictor FIR
-
+
10

FIG. 2D

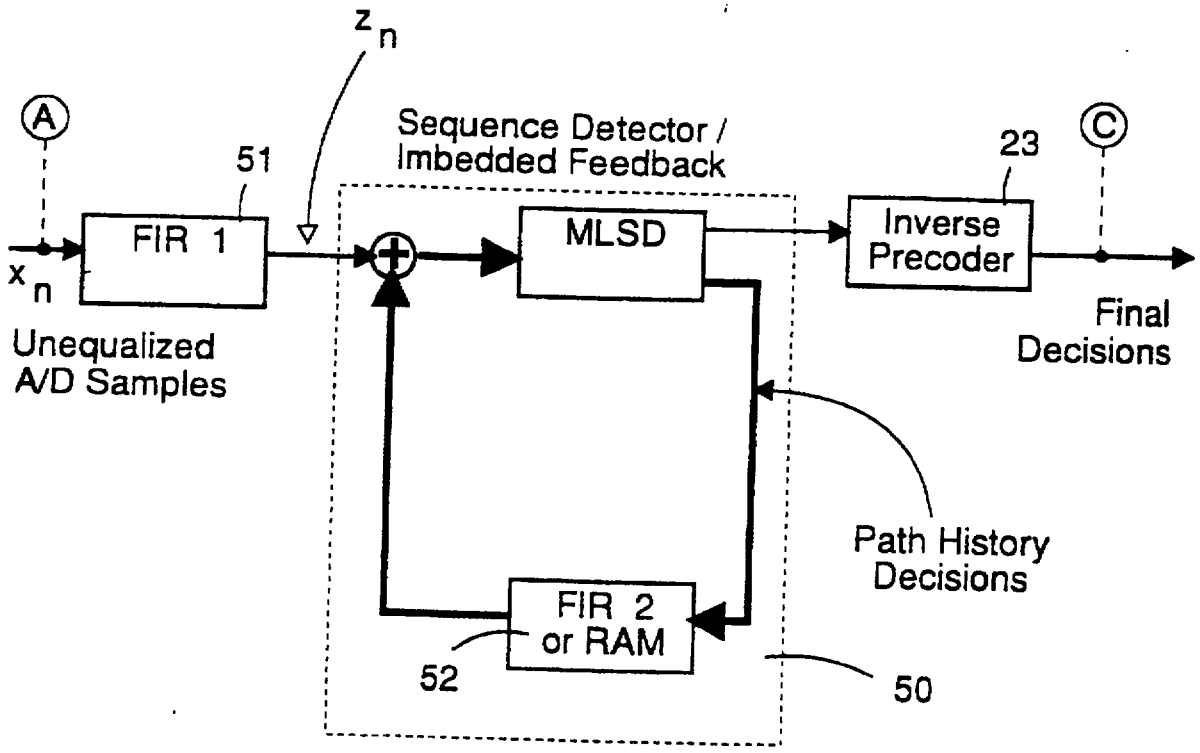

z n
A
Sequence Detector /
Imbedded Feedback
51
23
C
FIR 1
MLSD
Inverse
Precoder
x n
Unequalized
A/D Samples
Final
Decisions
Path History
Decisions
FIR 2
or RAM
52
50

FIG. 2E

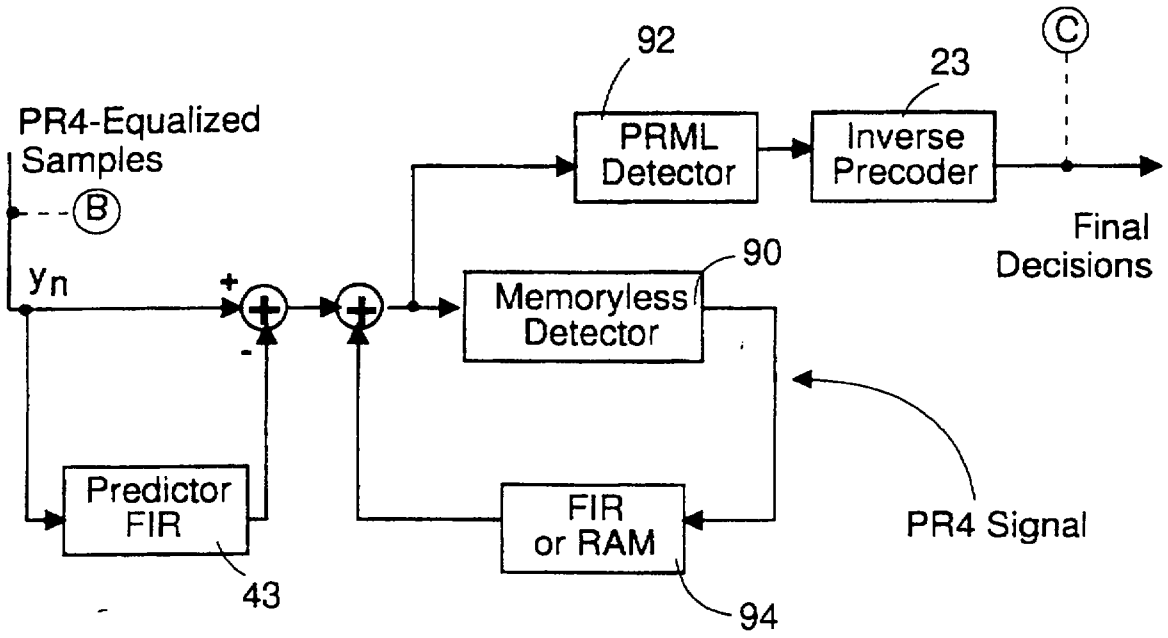

PR4-Equalized
Samples
B
yn
+
-
92
PRML
Detector
23
Inverse
Precoder
C
Final
Decisions
90
Memoryless
Detector
Predictor
FIR
43
FIR
or RAM
94
PR4 Signal

FIG. 3A

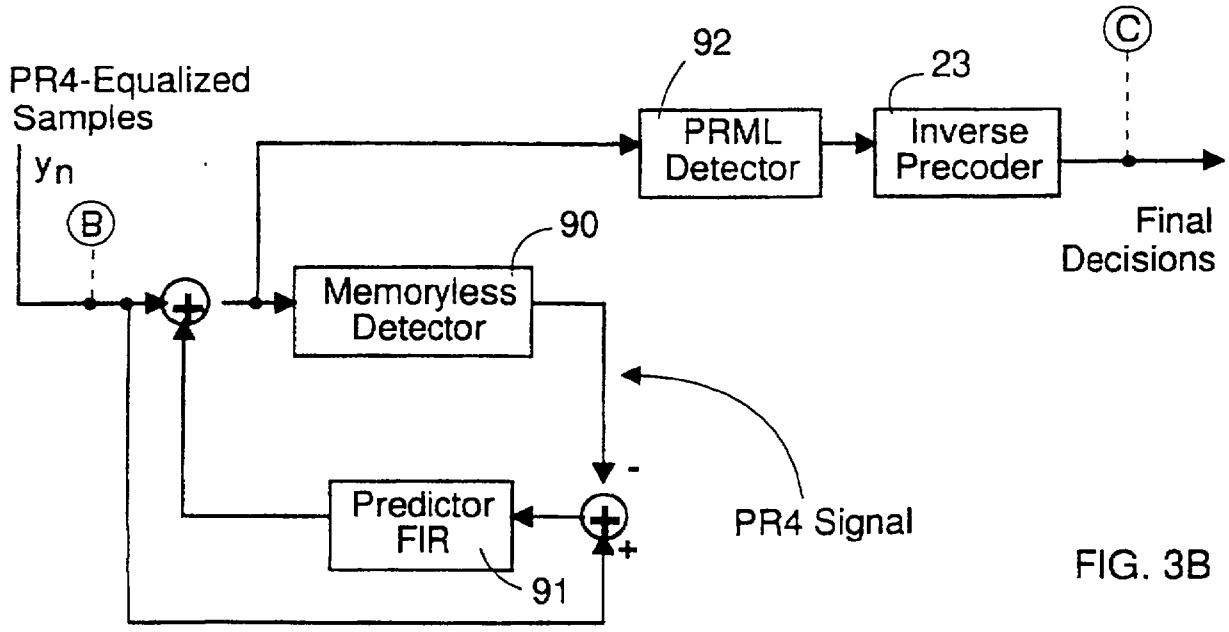

PR4-Equalized
Samples
yn
B
92
PRML
Detector
23
Inverse
Precoder
C
Final
Decisions
90
Memoryless
Detector
-
Predictor
FIR
+
91
PR4 Signal

FIG. 3B

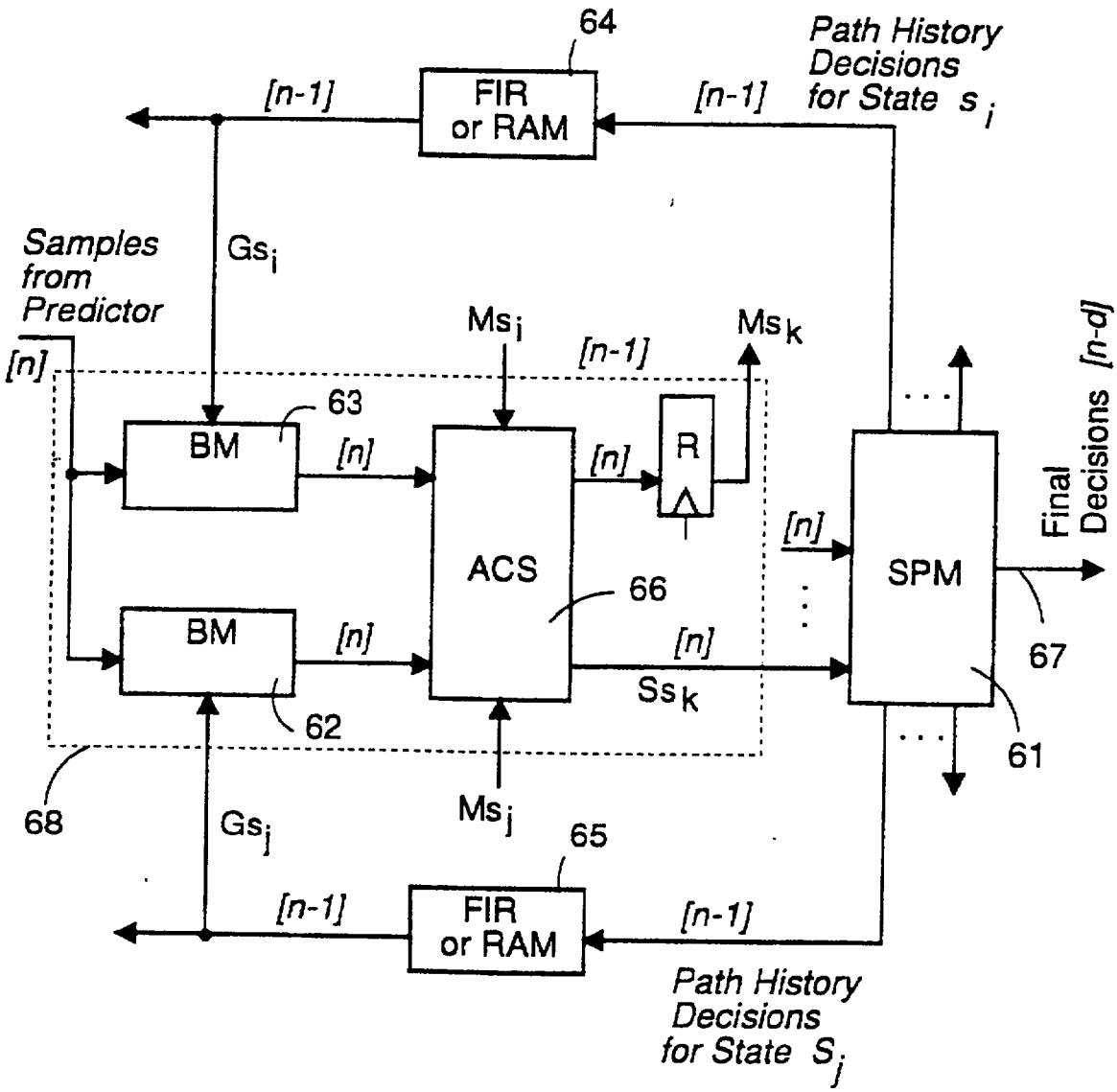

64
Path History Decisions for State s_i
[n-1]
FIR or RAM
[n-1]
Samples from Predictor
Gs_i
Ms_i
[n-1]
Ms_k
[n]
63
BM
[n]
ACS
[n]
R
66
[n]
SPM
Final Decisions [n-d]
67
BM
[n]
[n]
Ss_k
62
61
68
Gs_j
Ms_j
65
[n-1]
FIR or RAM
[n-1]
Path History Decisions for State S_j

FIG. 4

NPML : 2-State Trellis

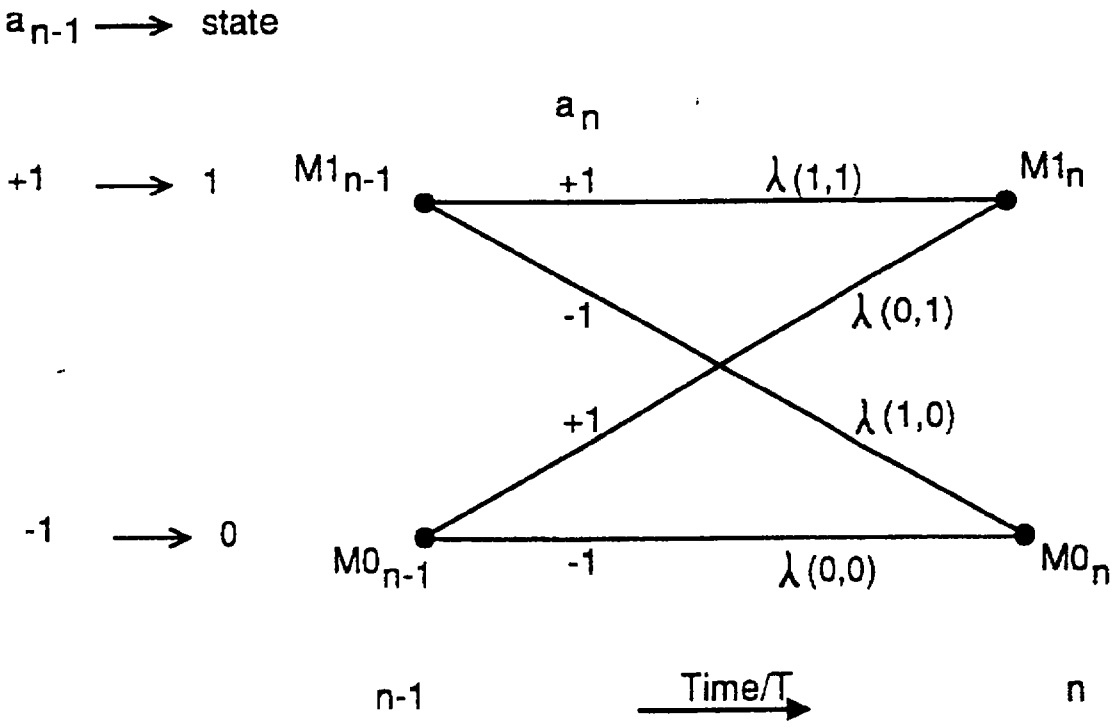


FIG. 5

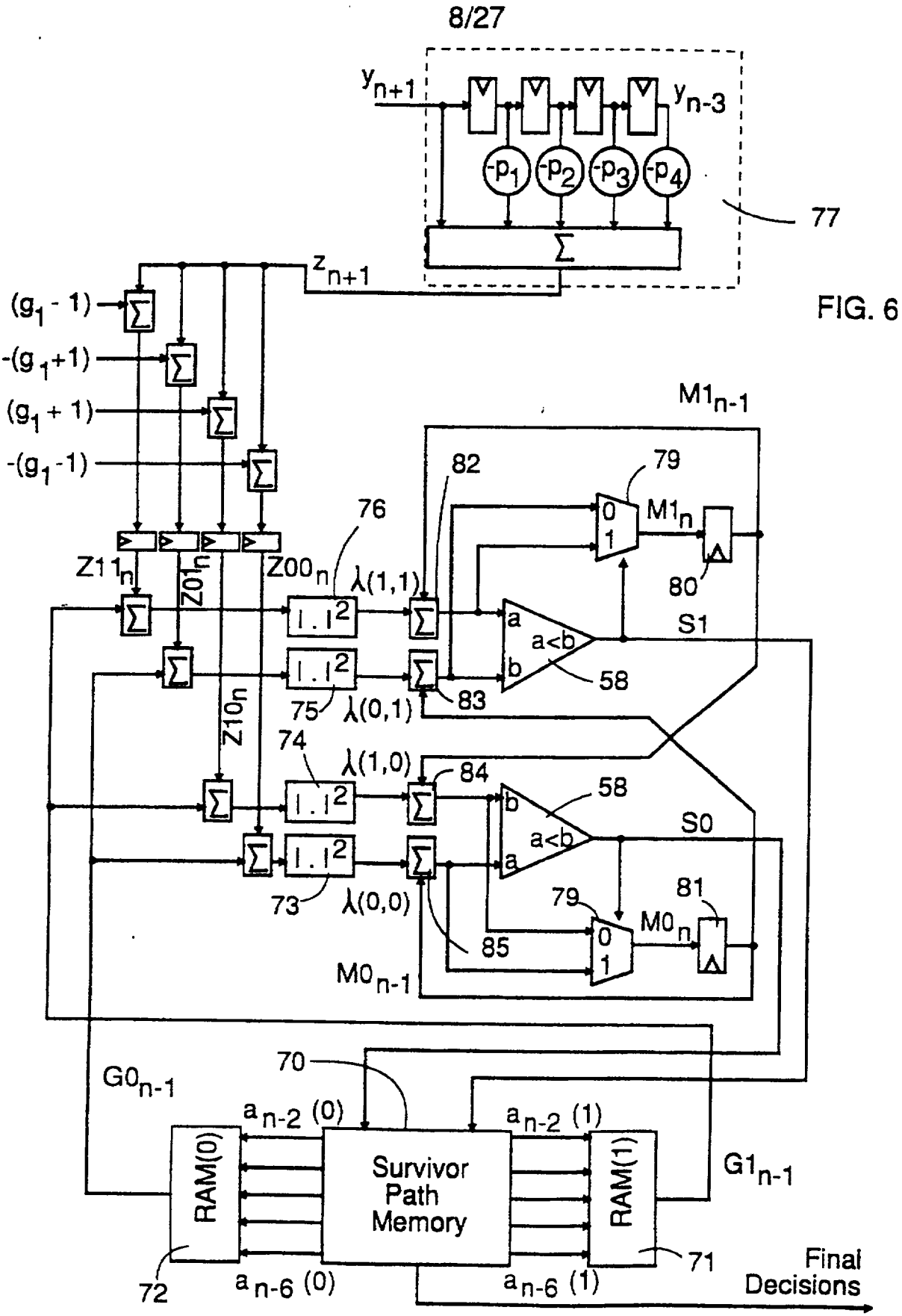

y_{n+1}
y_{n-3}
$-p_1$
$-p_2$
$-p_3$
$-p_4$
77
z_{n+1}
$(g_1 - 1)$
$-(g_1+1)$
$(g_1 + 1)$
$-(g_1-1)$
$M1_{n-1}$
82
79
76
$M1_n$
$Z11_n$
$Z01_n$
$Z00_n$
$\lambda(1,1)$
80
S1
58
83
75
$\lambda(0,1)$
$Z10_n$
74
$\lambda(1,0)$
84
58
S0
73
$\lambda(0,0)$
79
81
$M0_n$
85
$M0_{n-1}$
70
$G0_{n-1}$
a_{n-2} (0)
a_{n-2} (1)
RAM(0)
Survivor Path Memory
RAM(1)
$G1_{n-1}$
72
a_{n-6} (0)
a_{n-6} (1)
71
Final Decisions

FIG. 6

NPML : 2-State Trellis (Difference Metric)

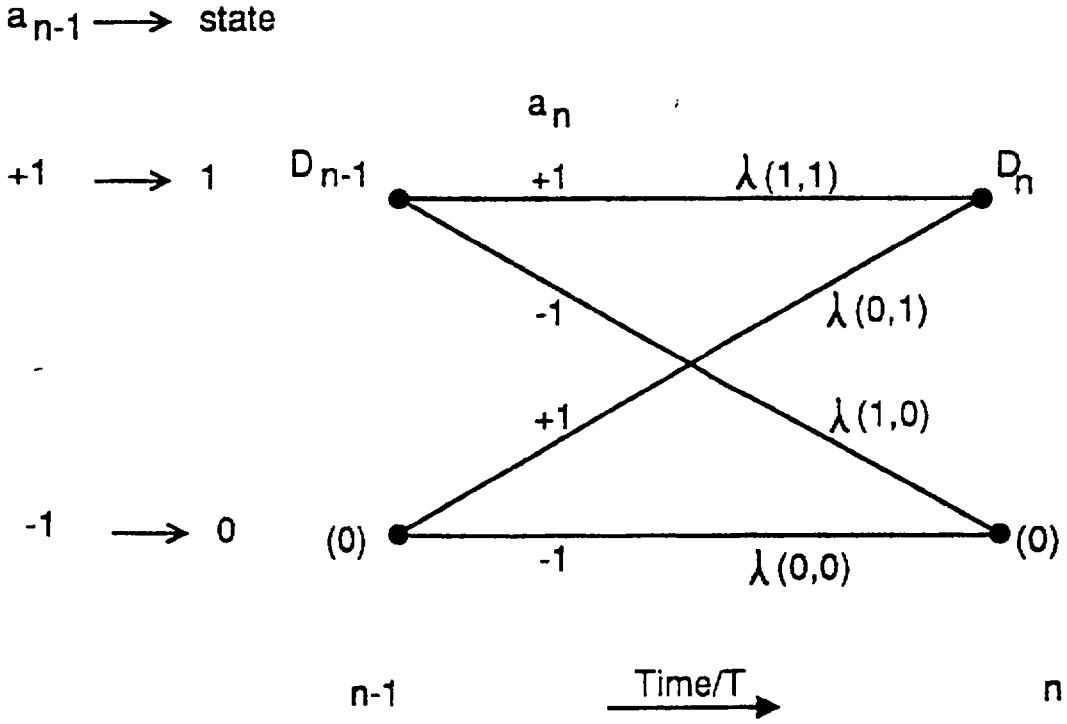


FIG. 7

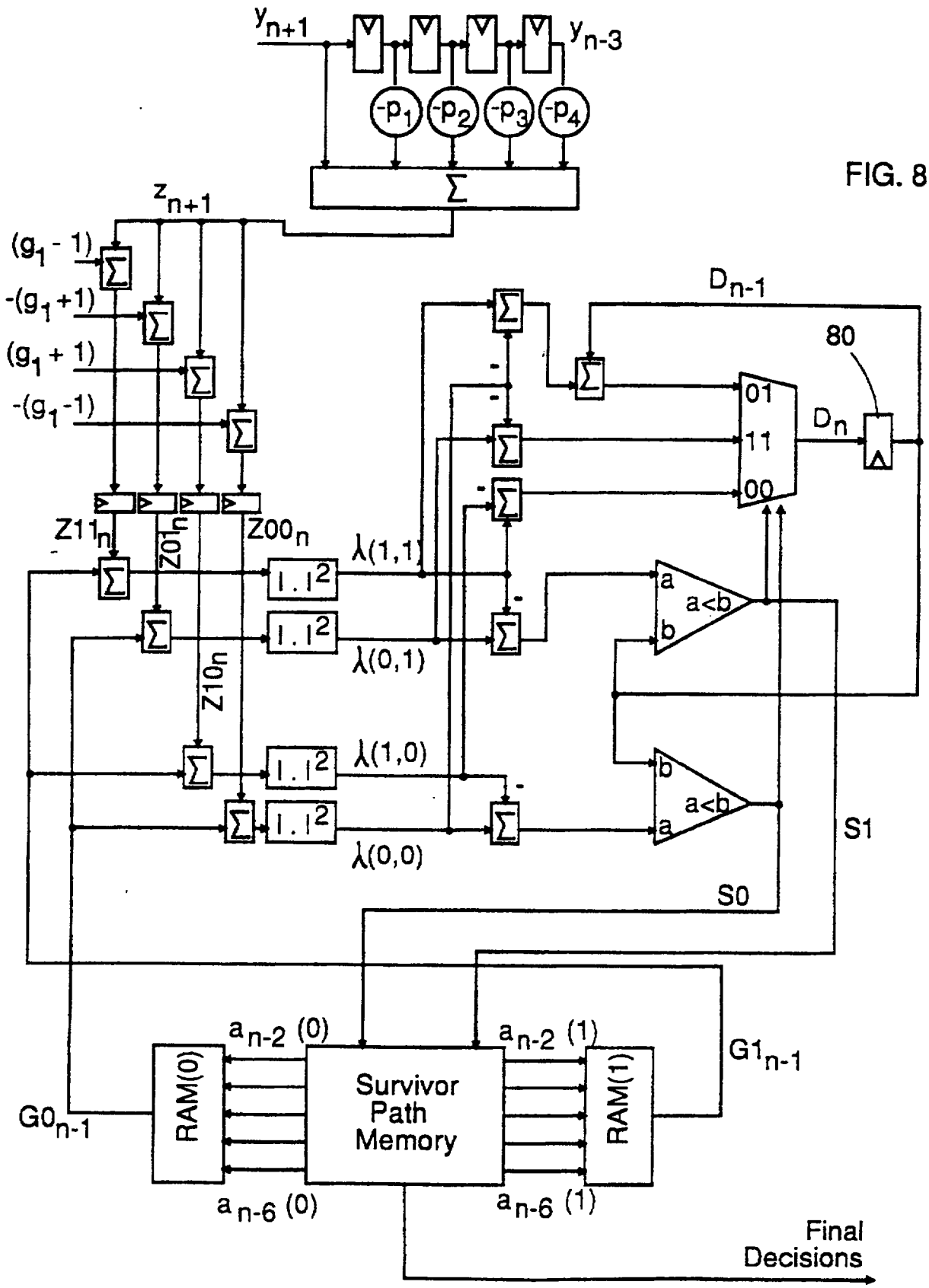

y_{n+1}
y_{n-3}
$-p_1$
$-p_2$
$-p_3$
$-p_4$
Σ
z_{n+1}
$(g_1 - 1)$
$-(g_1+1)$
$(g_1 + 1)$
$-(g_1-1)$
D_{n-1}
80
01
11
00
D_n
$Z11_n$
$Z01_n$
$Z00_n$
$Z10_n$
$\lambda(1,1)$
$\lambda(0,1)$
$\lambda(1,0)$
$\lambda(0,0)$
$|.|^2$
a
b
a<b
S1
S0
a_{n-2} (0)
a_{n-2} (1)
$G1_{n-1}$
$G0_{n-1}$
RAM(0)
RAM(1)
Survivor Path Memory
a_{n-6} (0)
a_{n-6} (1)
Final Decisions

FIG. 8

NPML : 4-State Trellis

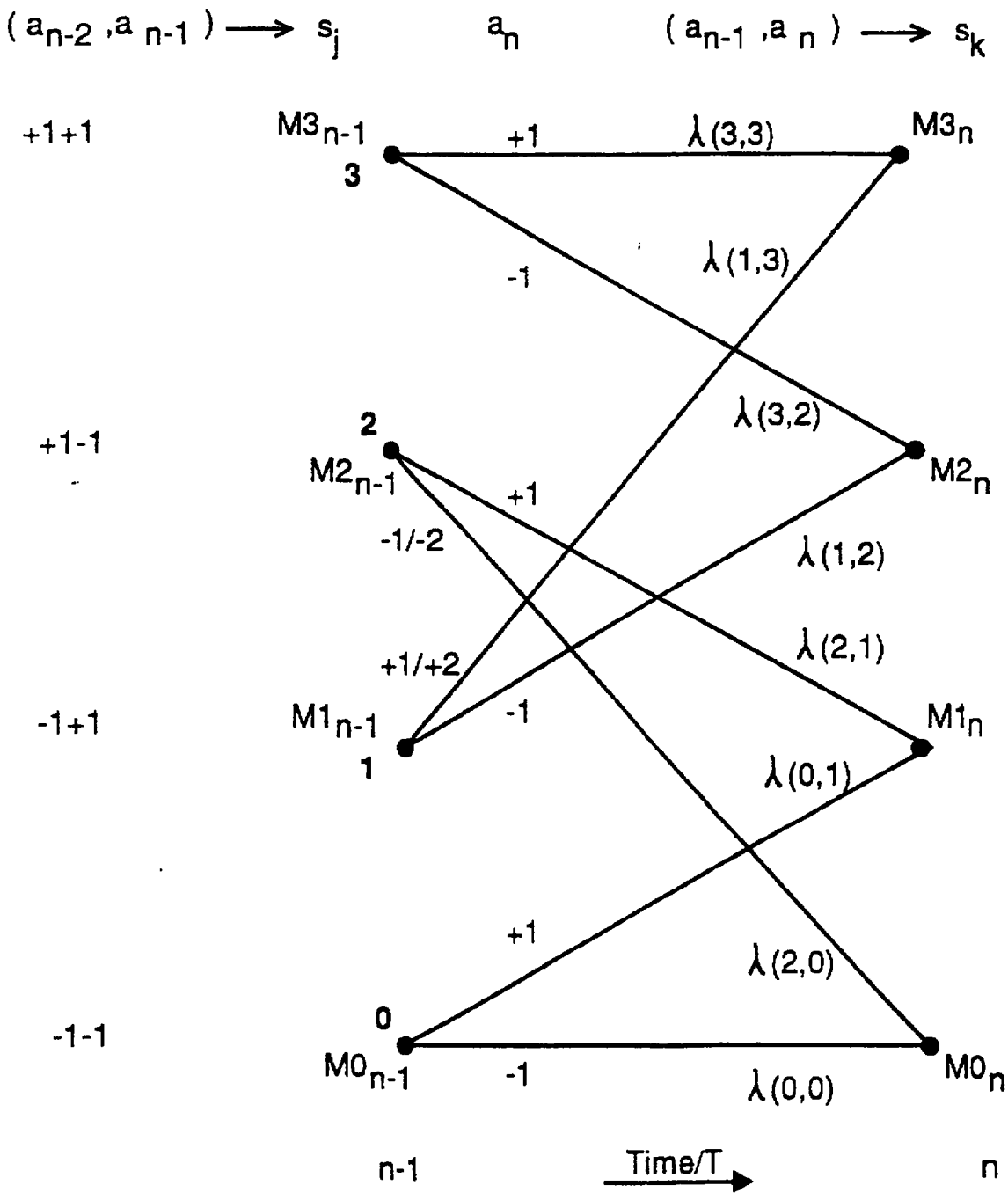


FIG. 9

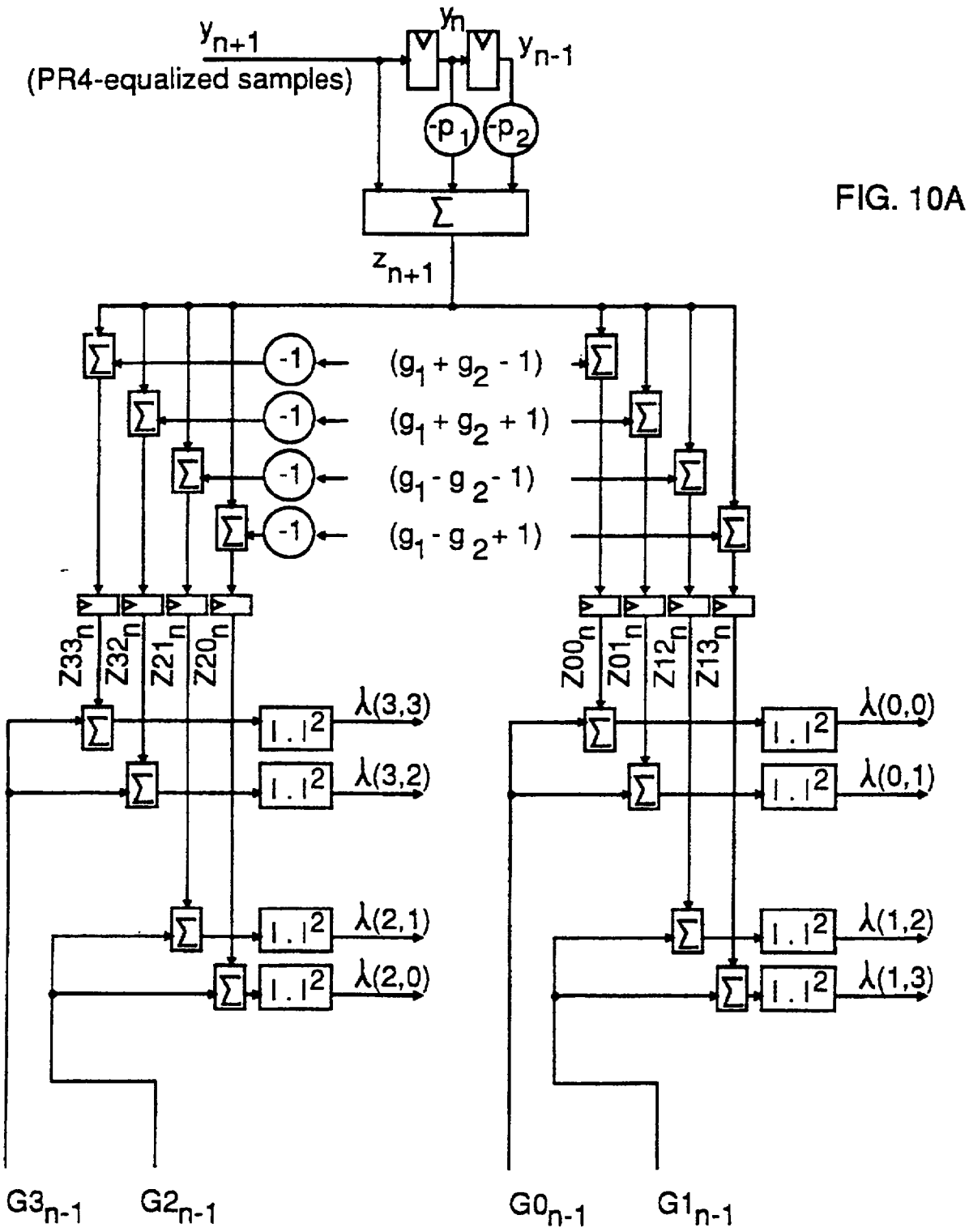

y_{n+1}
(PR4-equalized samples)
y_n
y_{n-1}
$-p_1$
$-p_2$
Σ
z_{n+1}
-1
$(g_1 + g_2 - 1)$
$(g_1 + g_2 + 1)$
$(g_1 - g_2 - 1)$
$(g_1 - g_2 + 1)$
$Z33_n$
$Z32_n$
$Z21_n$
$Z20_n$
$Z00_n$
$Z01_n$
$Z12_n$
$Z13_n$
$|.|^2$
$\lambda(3,3)$
$\lambda(3,2)$
$\lambda(2,1)$
$\lambda(2,0)$
$\lambda(0,0)$
$\lambda(0,1)$
$\lambda(1,2)$
$\lambda(1,3)$
$G3_{n-1}$
$G2_{n-1}$
$G0_{n-1}$
$G1_{n-1}$

FIG. 10A

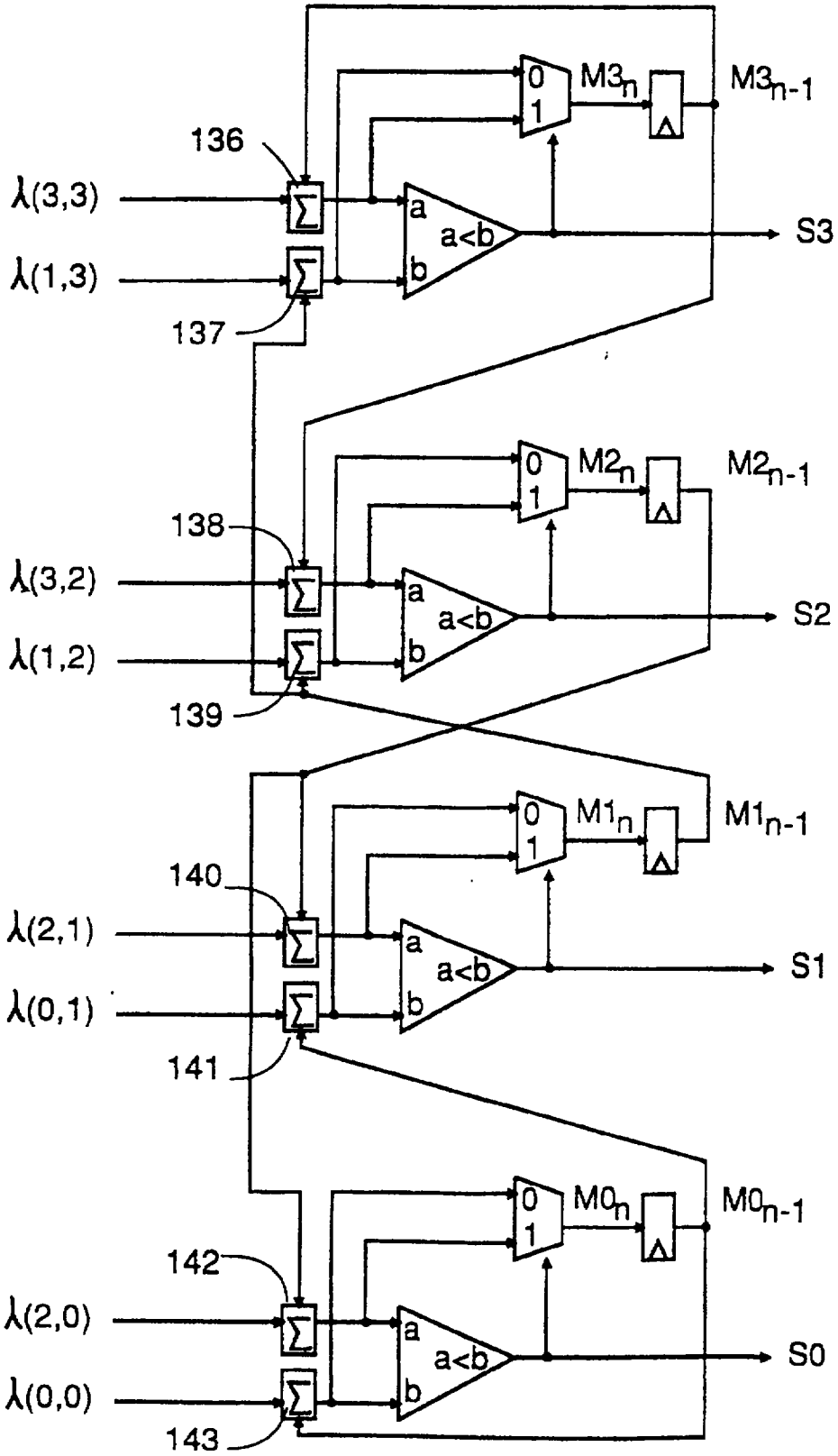

136
λ(3,3)
λ(1,3)
137
a
b
a<b
0
1
M3n
M3n-1
S3
138
λ(3,2)
λ(1,2)
139
M2n
M2n-1
S2
140
λ(2,1)
λ(0,1)
141
M1n
M1n-1
S1
142
λ(2,0)
λ(0,0)
143
M0n
M0n-1
S0

FIG. 10B

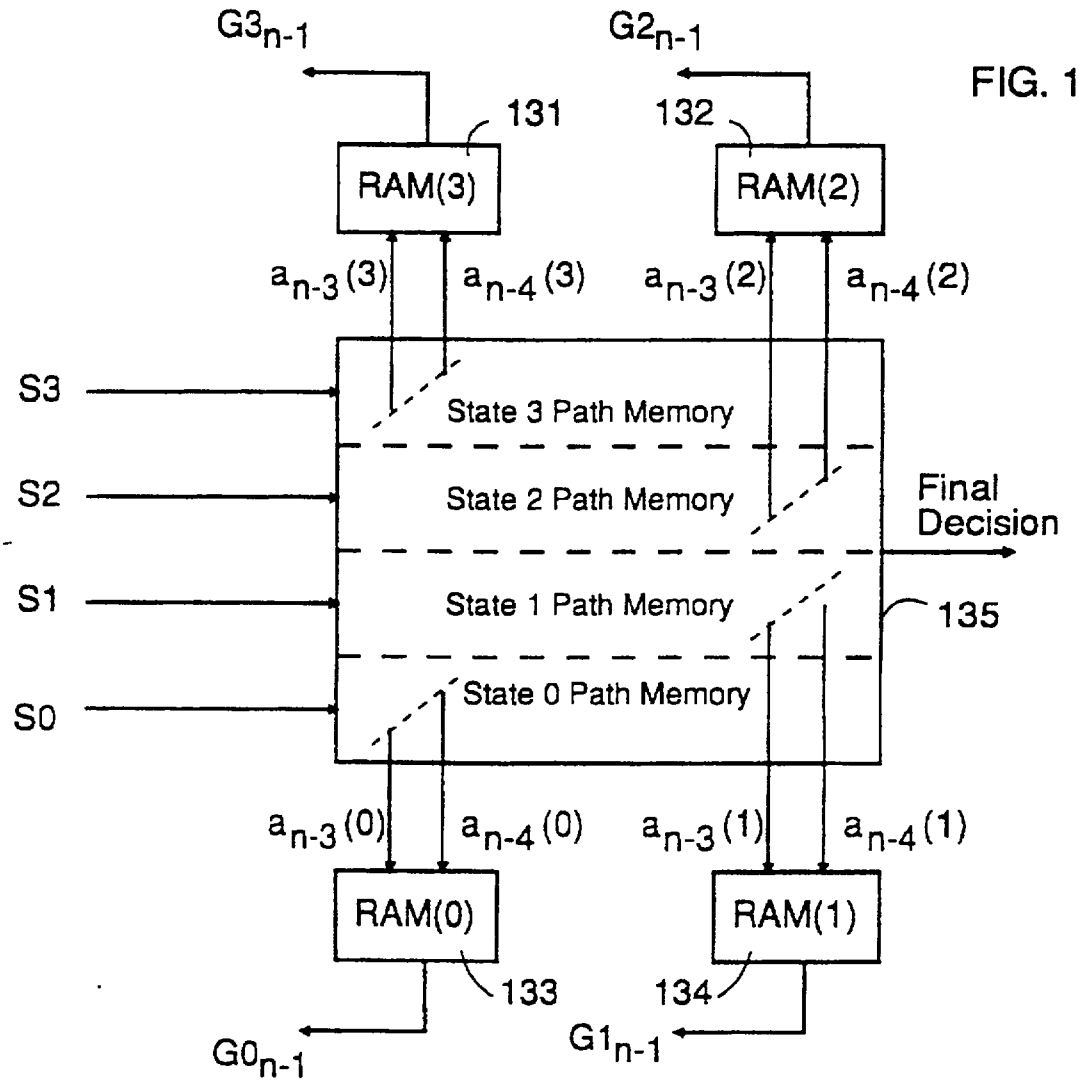

G3n-1
G2n-1
131
132
RAM(3)
RAM(2)
an-3(3)
an-4(3)
an-3(2)
an-4(2)
S3
S2
S1
S0
State 3 Path Memory
State 2 Path Memory
State 1 Path Memory
State 0 Path Memory
Final Decision
135
an-3(0)
an-4(0)
an-3(1)
an-4(1)
RAM(0)
RAM(1)
133
134
G0n-1
G1n-1

FIG. 10C

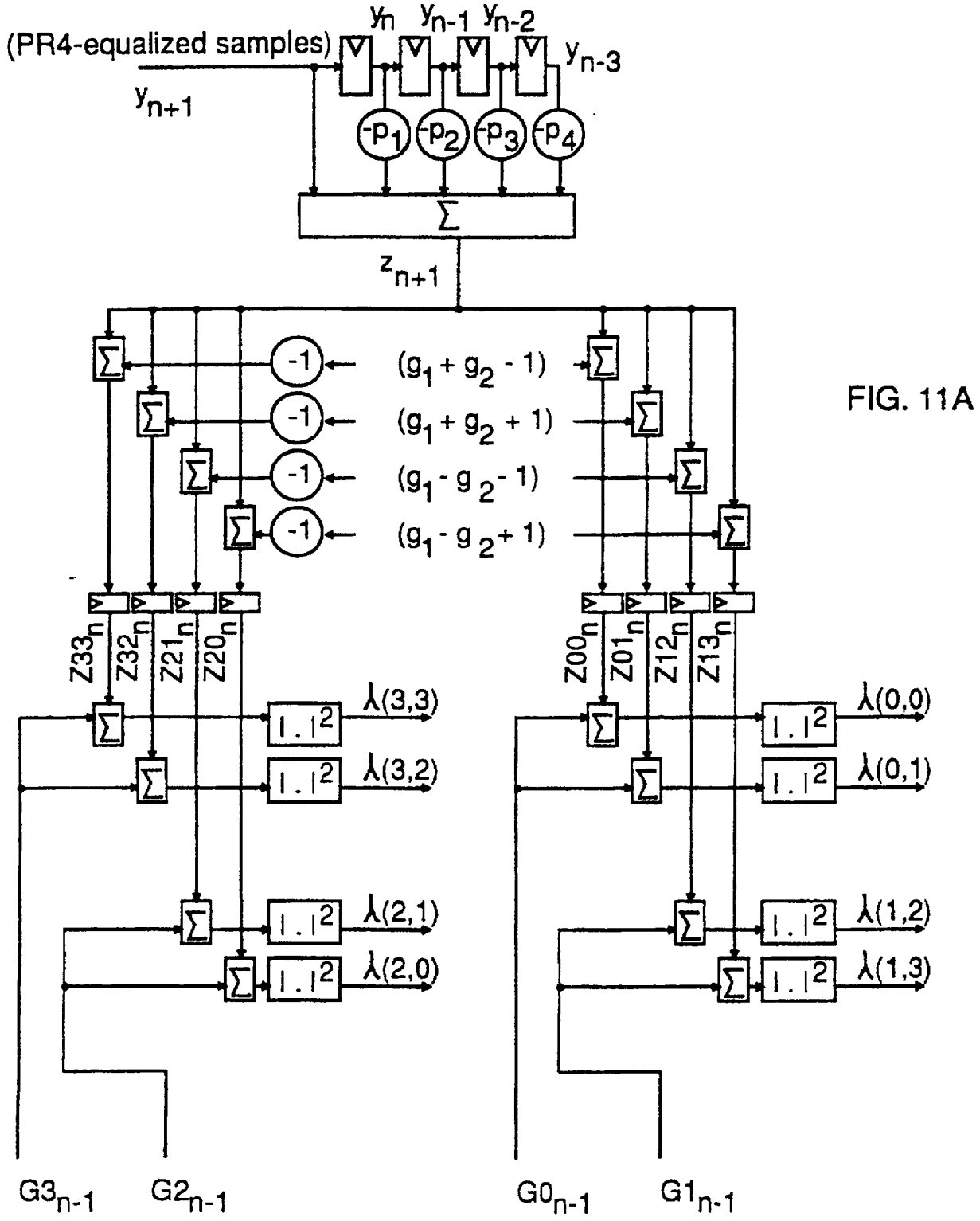

(PR4-equalized samples)
y_{n+1}
y_n y_{n-1} y_{n-2} y_{n-3}
$-p_1$ $-p_2$ $-p_3$ $-p_4$
Σ
z_{n+1}
-1 $(g_1 + g_2 - 1)$
-1 $(g_1 + g_2 + 1)$
-1 $(g_1 - g_2 - 1)$
-1 $(g_1 - g_2 + 1)$
$Z33_n$ $Z32_n$ $Z21_n$ $Z20_n$
$Z00_n$ $Z01_n$ $Z12_n$ $Z13_n$
$|.|^2$
$\lambda(3,3)$ $\lambda(3,2)$ $\lambda(2,1)$ $\lambda(2,0)$
$\lambda(0,0)$ $\lambda(0,1)$ $\lambda(1,2)$ $\lambda(1,3)$
$G3_{n-1}$ $G2_{n-1}$ $G0_{n-1}$ $G1_{n-1}$

FIG. 11A

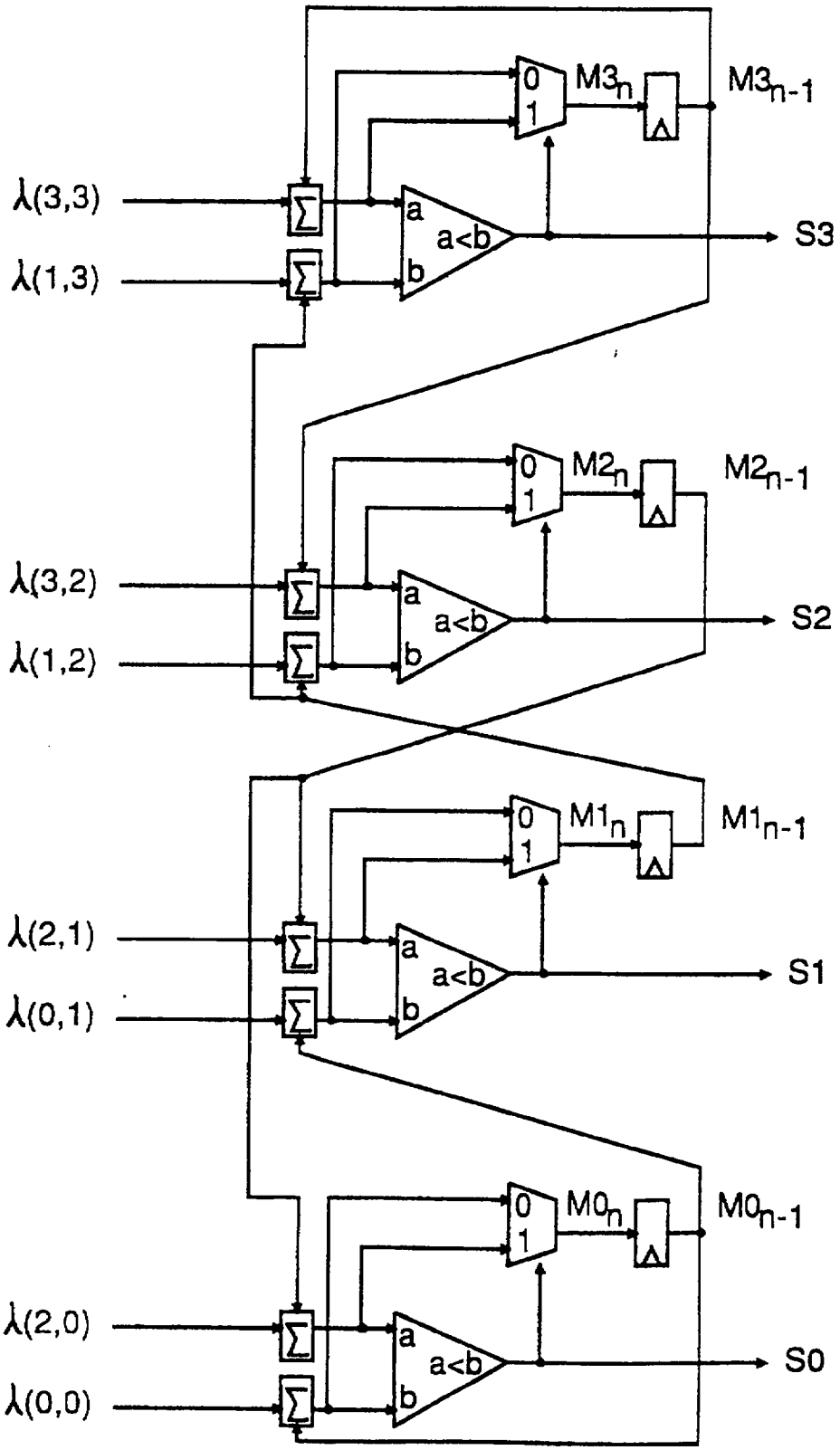
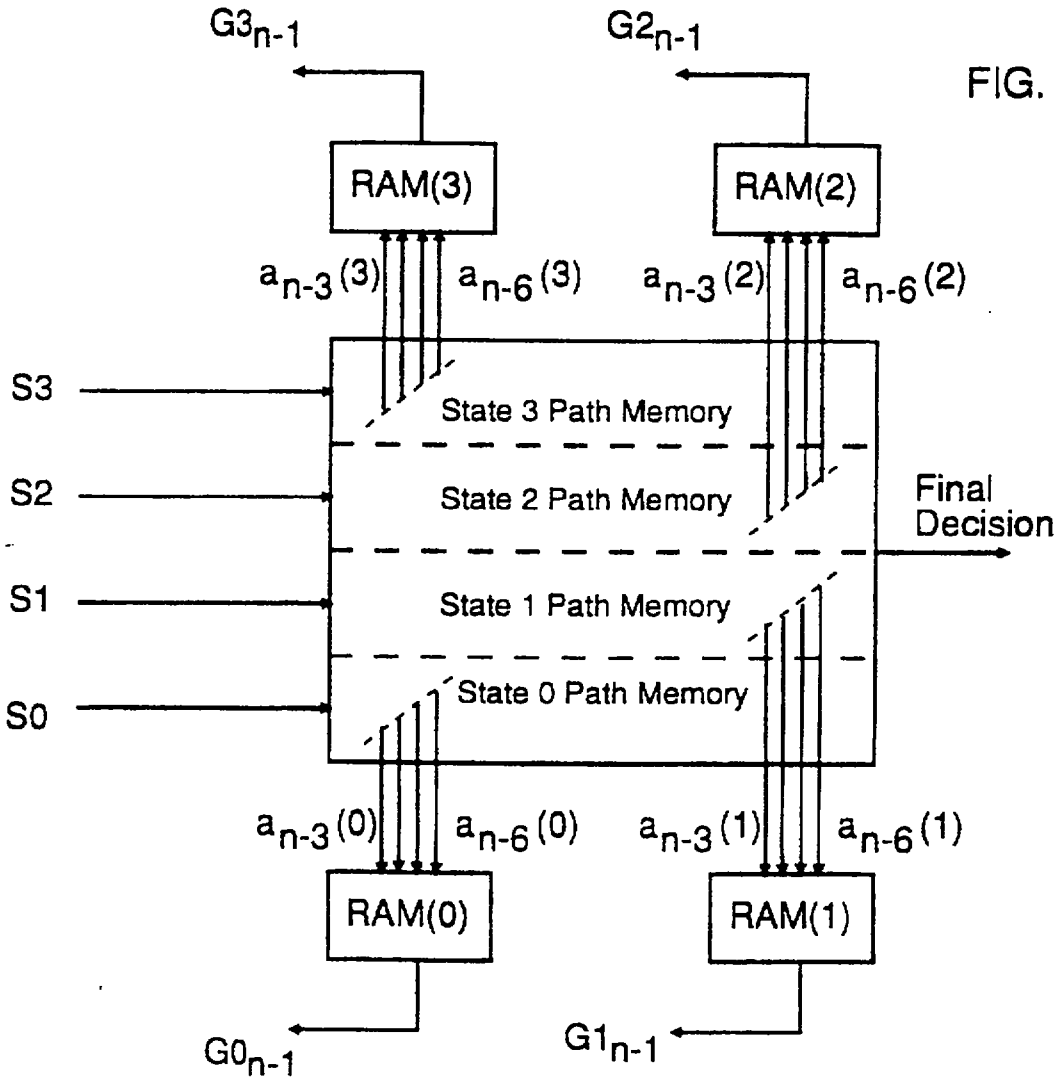

λ(3,3)
λ(1,3)
λ(3,2)
λ(1,2)
λ(2,1)
λ(0,1)
λ(2,0)
λ(0,0)
Σ
a
b
a<b
0
1
M3n
M3n-1
M2n
M2n-1
M1n
M1n-1
M0n
M0n-1
S3
S2
S1
S0

FIG. 11B

FIG. 11C


G3n-1
G2n-1
RAM(3)
RAM(2)
an-3 (3)
an-6 (3)
an-3 (2)
an-6 (2)
S3
S2
S1
S0
State 3 Path Memory
State 2 Path Memory
State 1 Path Memory
State 0 Path Memory
Final Decision
an-3 (0)
an-6 (0)
an-3 (1)
an-6 (1)
RAM(0)
RAM(1)
G0n-1
G1n-1

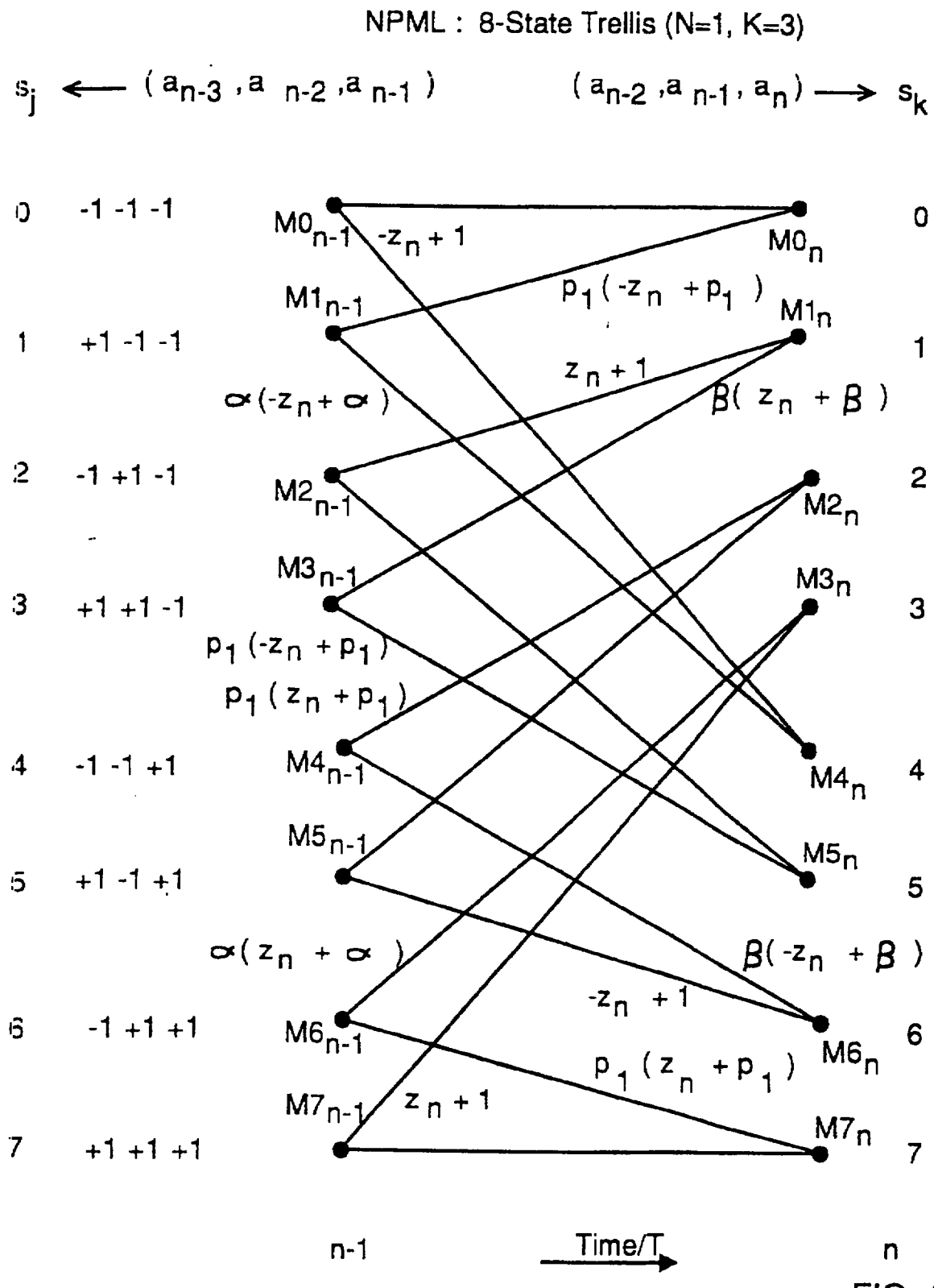

NPML : 8-State Trellis (N=1, K=3)
s_j ← (a_{n-3} , a_{n-2} , a_{n-1})
(a_{n-2} , a_{n-1} , a_n) → s_k
0 -1 -1 -1
1 +1 -1 -1
2 -1 +1 -1
3 +1 +1 -1
4 -1 -1 +1
5 +1 -1 +1
6 -1 +1 +1
7 +1 +1 +1
$M0_{n-1}$
$M1_{n-1}$
$M2_{n-1}$
$M3_{n-1}$
$M4_{n-1}$
$M5_{n-1}$
$M6_{n-1}$
$M7_{n-1}$
$M0_n$
$M1_n$
$M2_n$
$M3_n$
$M4_n$
$M5_n$
$M6_n$
$M7_n$
$-z_n + 1$
$p_1(-z_n + p_1)$
$z_n + 1$
$\alpha(-z_n + \alpha)$
$\beta(z_n + \beta)$
$p_1(-z_n + p_1)$
$p_1(z_n + p_1)$
$\alpha(z_n + \alpha)$
$\beta(-z_n + \beta)$
$-z_n + 1$
$p_1(z_n + p_1)$
$z_n + 1$
0 1 2 3 4 5 6 7
n-1
Time/T
n

FIG. 12

NPML : Transformed 8-State Trellis (N=1, K=3)

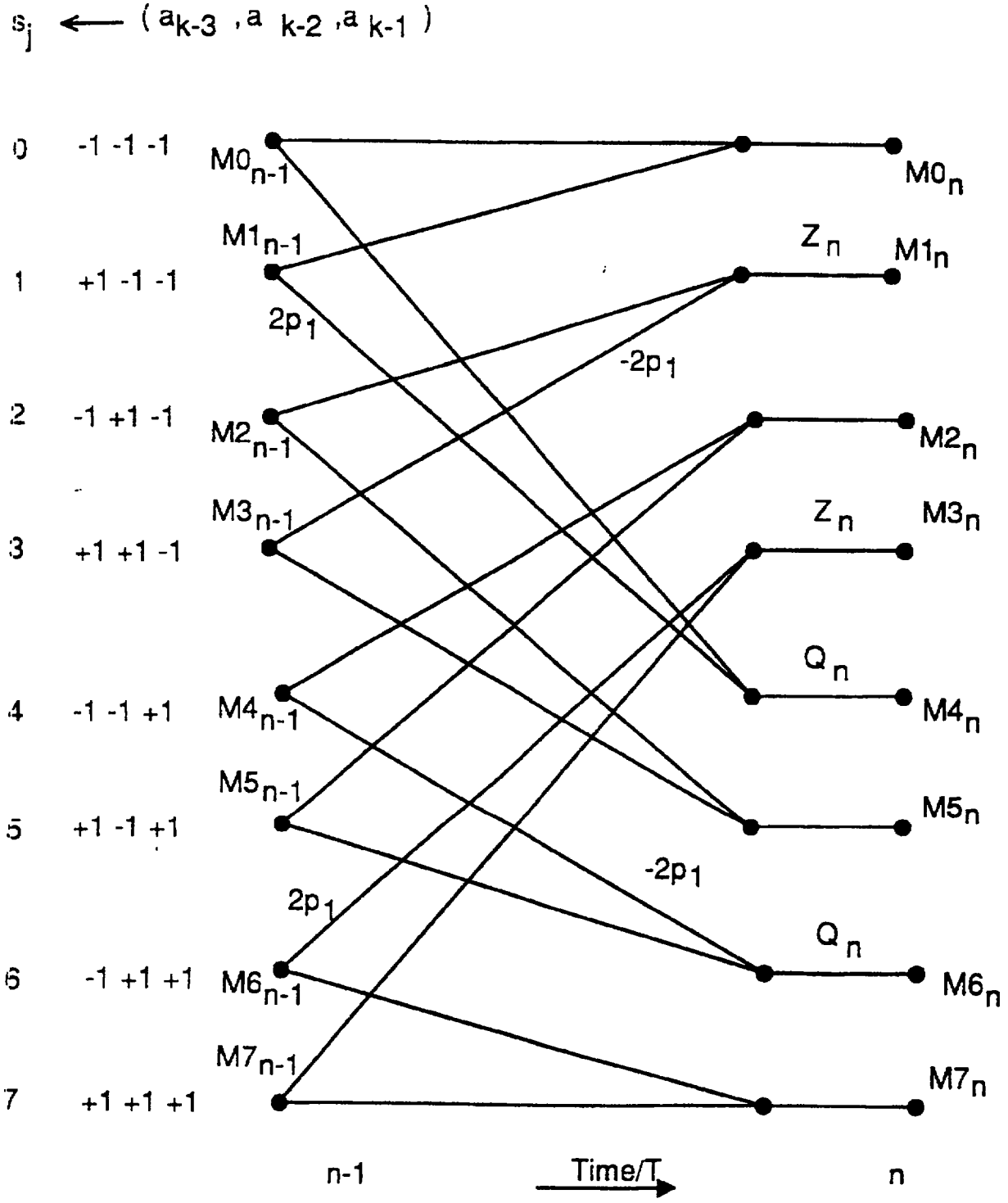


FIG. 13

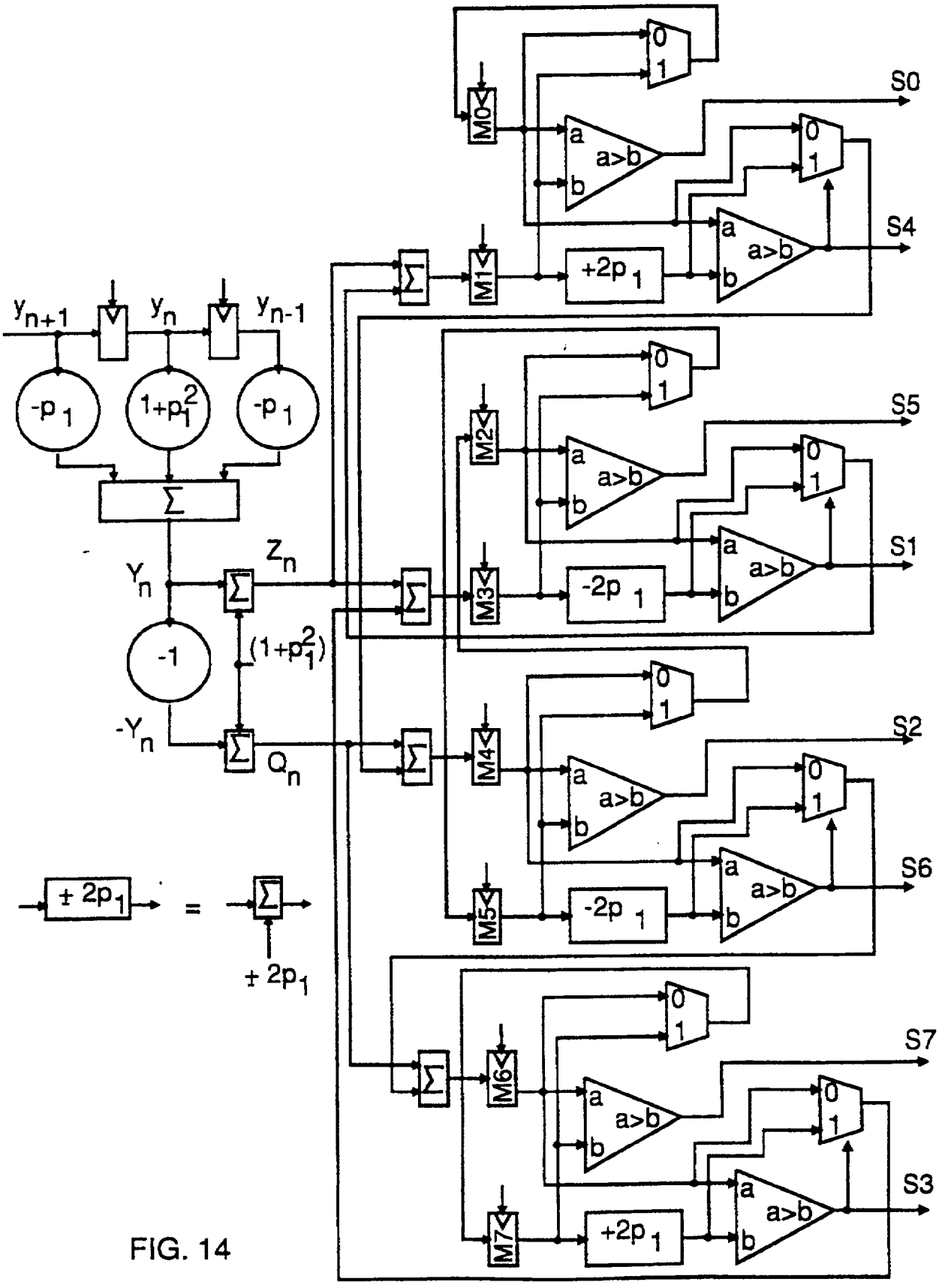

y_{n+1}
y_n
y_{n-1}
$-p_1$
$1+p_1^2$
$-p_1$
Y_n
Z_n
-1
$(1+p_1^2)$
$-Y_n$
Q_n
$\pm 2p_1$ = $\pm 2p_1$
M0
M1
M2
M3
M4
M5
M6
M7
a
b
a>b
0
1
$+2p_1$
$-2p_1$
S0
S4
S5
S1
S2
S6
S7
S3

FIG. 14

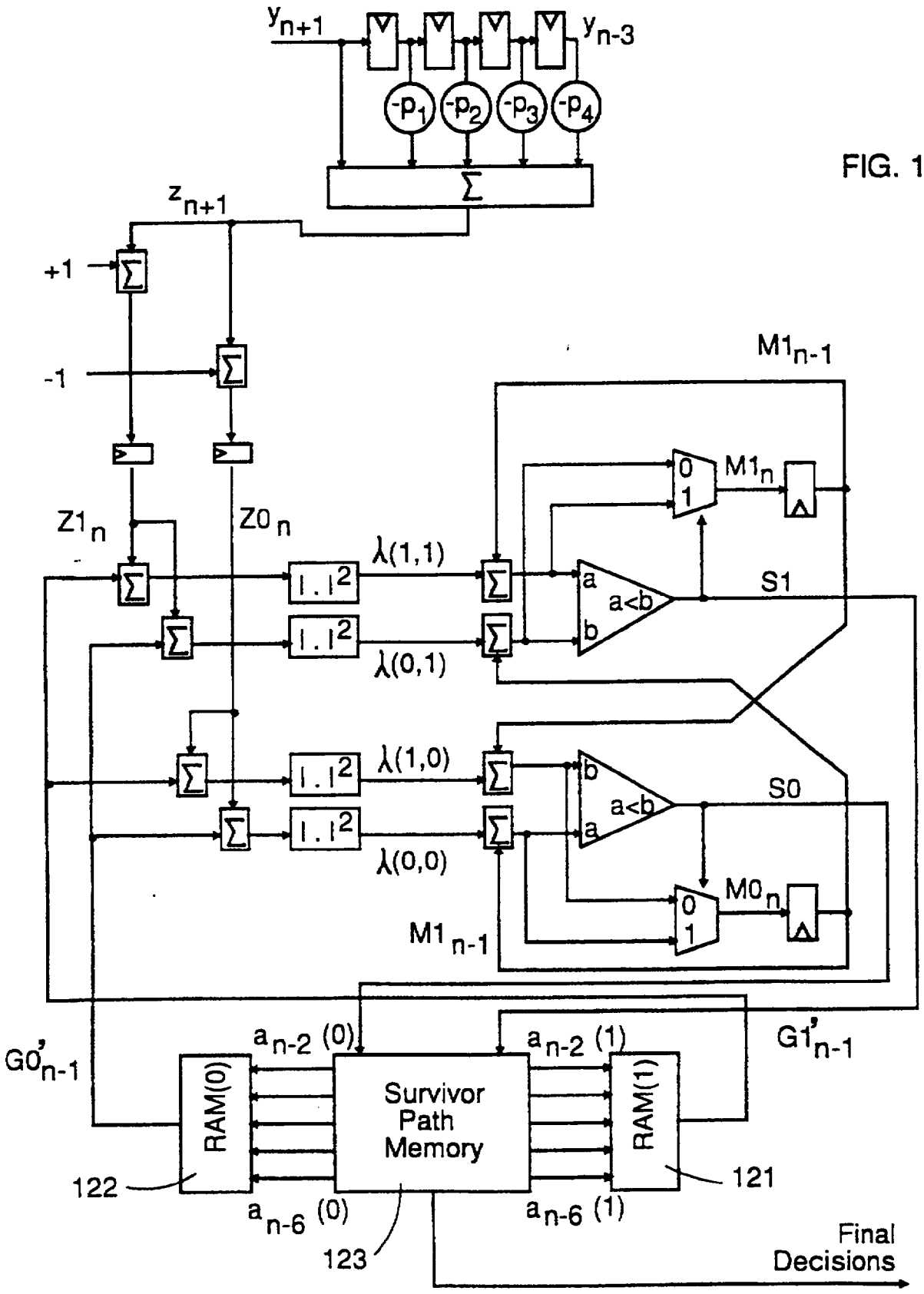

y_{n+1}
y_{n-3}
$-p_1$
$-p_2$
$-p_3$
$-p_4$
Σ
z_{n+1}
+1
-1
$M1_{n-1}$
$M1_n$
$Z1_n$
$Z0_n$
$\lambda(1,1)$
$\lambda(0,1)$
$\lambda(1,0)$
$\lambda(0,0)$
$|.|^2$
a
b
a<b
S1
S0
$M0_n$
$M1_{n-1}$
$G0'_{n-1}$
$G1'_{n-1}$
a_{n-2} (0)
a_{n-2} (1)
RAM(0)
RAM(1)
Survivor Path Memory
122
121
123
a_{n-6} (0)
a_{n-6} (1)
Final Decisions

FIG. 15

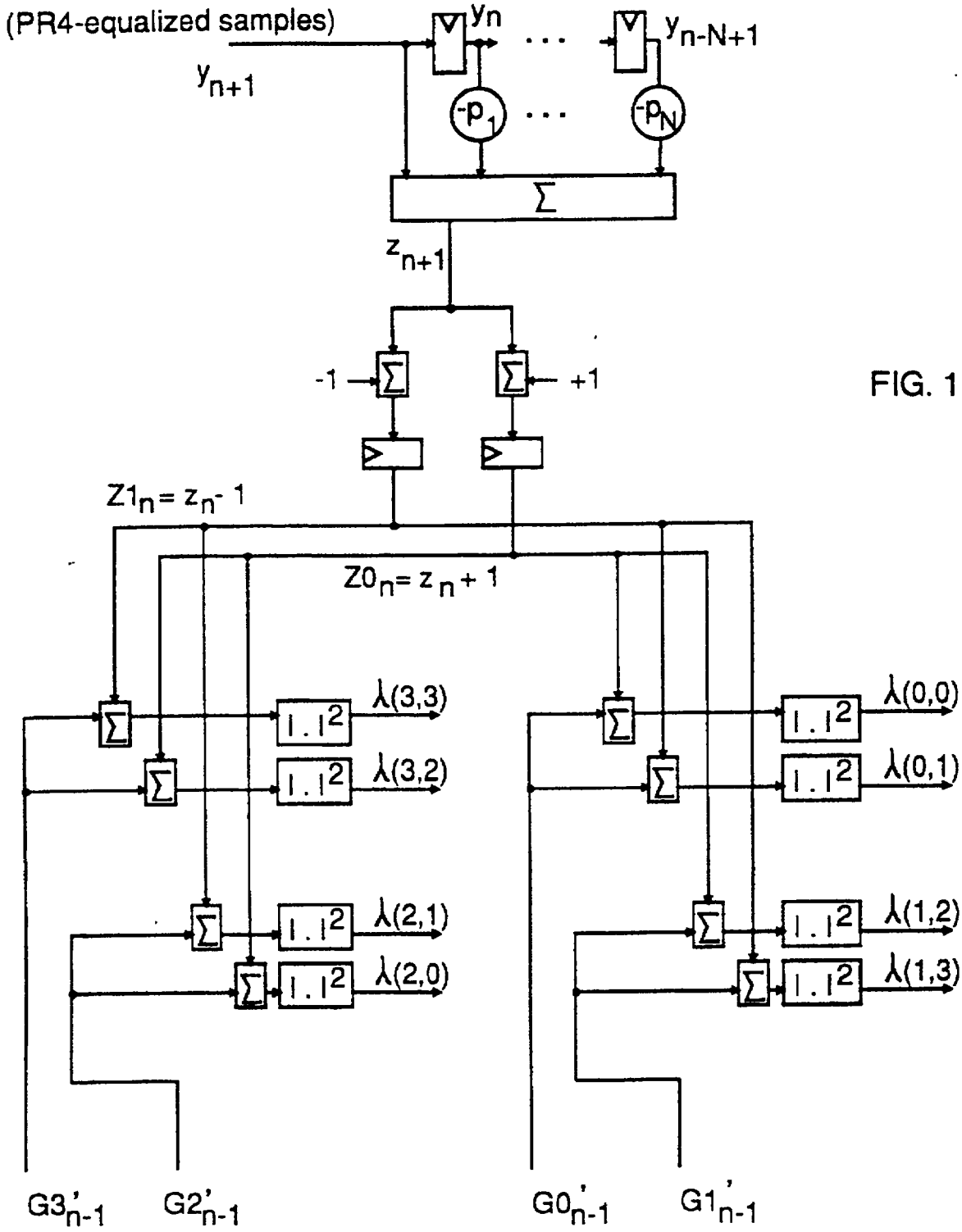

(PR4-equalized samples)
y_{n+1}
y_n
y_{n-N+1}
$-p_1$
$-p_N$
Σ
z_{n+1}
-1
+1
$Z1_n = z_n - 1$
$Z0_n = z_n + 1$
$|.|^2$
$\lambda(3,3)$
$\lambda(3,2)$
$\lambda(2,1)$
$\lambda(2,0)$
$\lambda(0,0)$
$\lambda(0,1)$
$\lambda(1,2)$
$\lambda(1,3)$
$G3'_{n-1}$
$G2'_{n-1}$
$G0'_{n-1}$
$G1'_{n-1}$

FIG. 16A

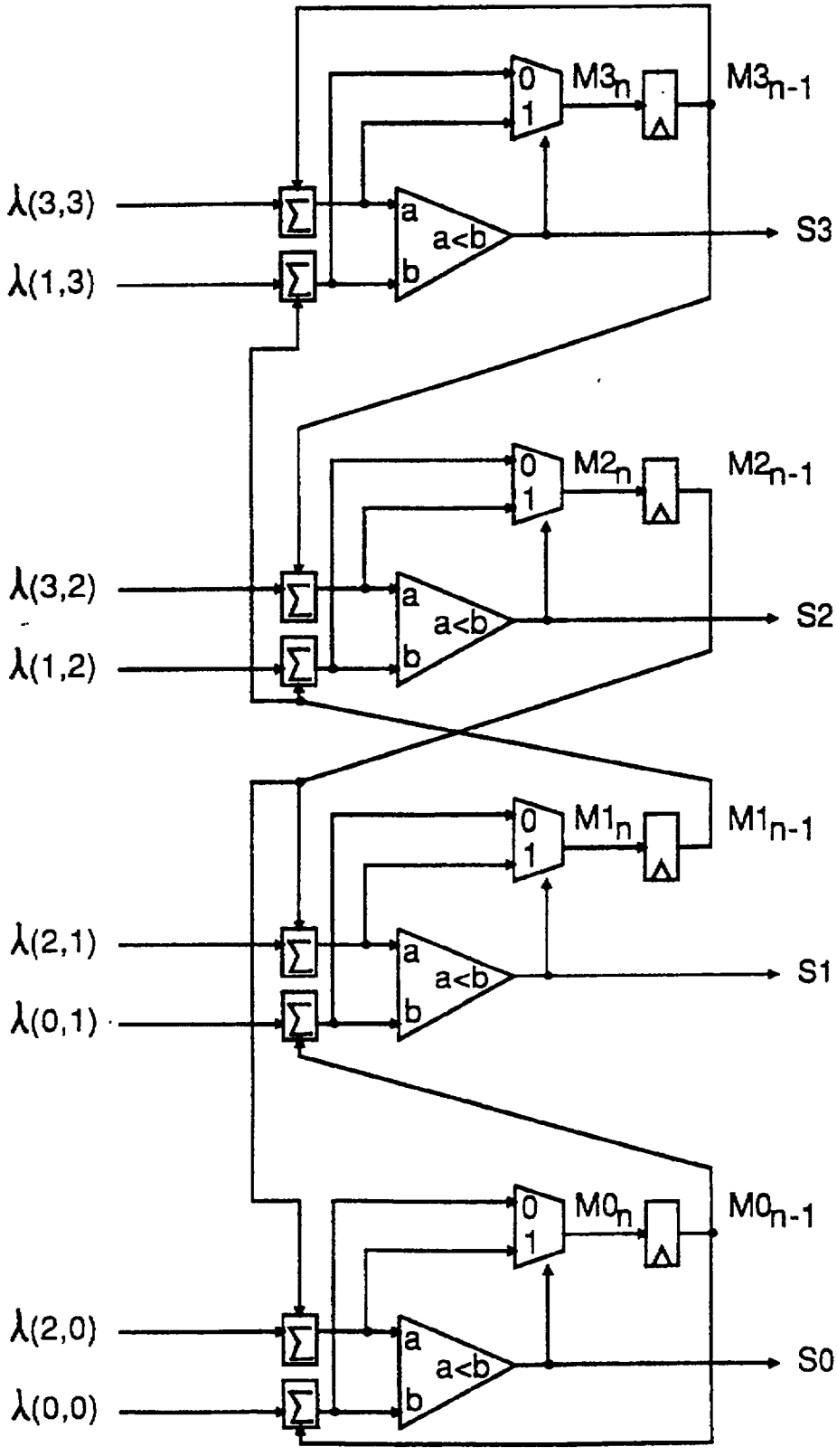

λ(3,3)
λ(1,3)
λ(3,2)
λ(1,2)
λ(2,1)
λ(0,1)
λ(2,0)
λ(0,0)
a
b
a<b
0
1
M3n
M3n-1
M2n
M2n-1
M1n
M1n-1
M0n
M0n-1
S3
S2
S1
S0

FIG. 16B

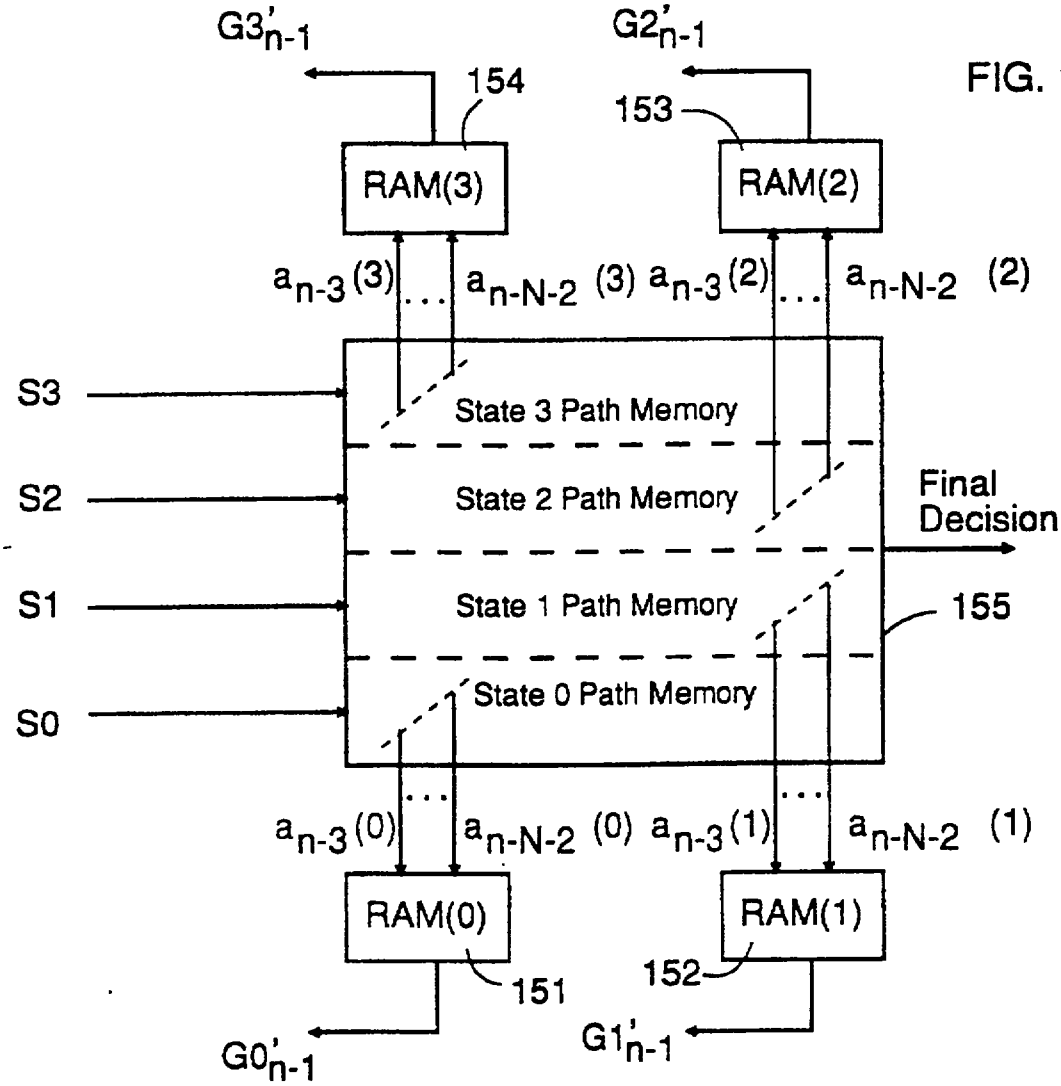

G3'n-1
G2'n-1
154
153
RAM(3)
RAM(2)
an-3 (3) ... an-N-2 (3)
an-3 (2) ... an-N-2 (2)
S3
S2
S1
S0
State 3 Path Memory
State 2 Path Memory
State 1 Path Memory
State 0 Path Memory
Final Decision
155
an-3 (0) ... an-N-2 (0)
an-3 (1) ... an-N-2 (1)
RAM(0)
RAM(1)
151
152
G0'n-1
G1'n-1

FIG. 16C

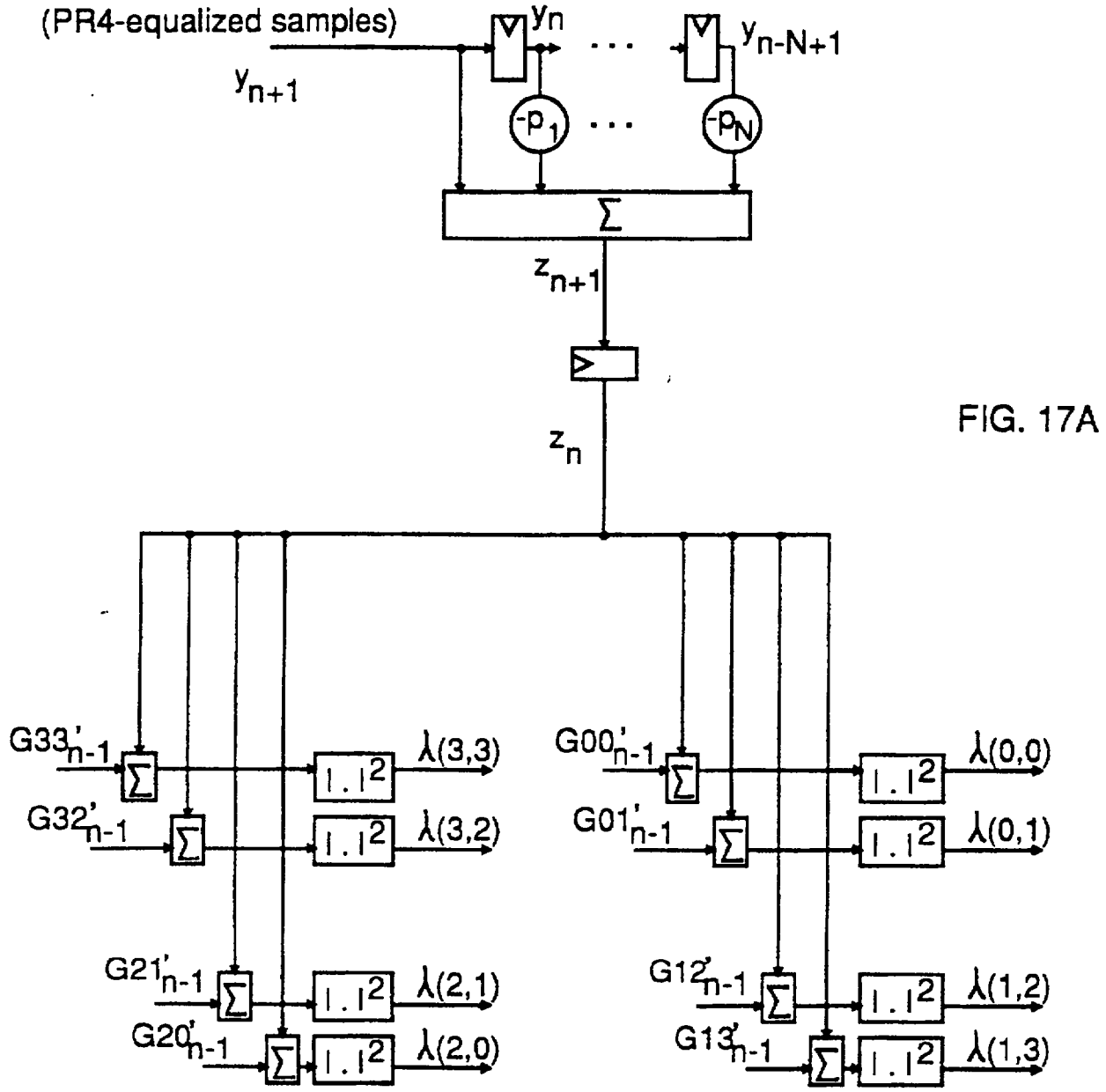

(PR4-equalized samples)
y_{n+1}
y_n
y_{n-N+1}
$-p_1$
$-p_N$
Σ
z_{n+1}
z_n
$G33'_{n-1}$
$G32'_{n-1}$
$G21'_{n-1}$
$G20'_{n-1}$
$G00'_{n-1}$
$G01'_{n-1}$
$G12'_{n-1}$
$G13'_{n-1}$
$|.|^2$
$\lambda(3,3)$
$\lambda(3,2)$
$\lambda(2,1)$
$\lambda(2,0)$
$\lambda(0,0)$
$\lambda(0,1)$
$\lambda(1,2)$
$\lambda(1,3)$

FIG. 17A

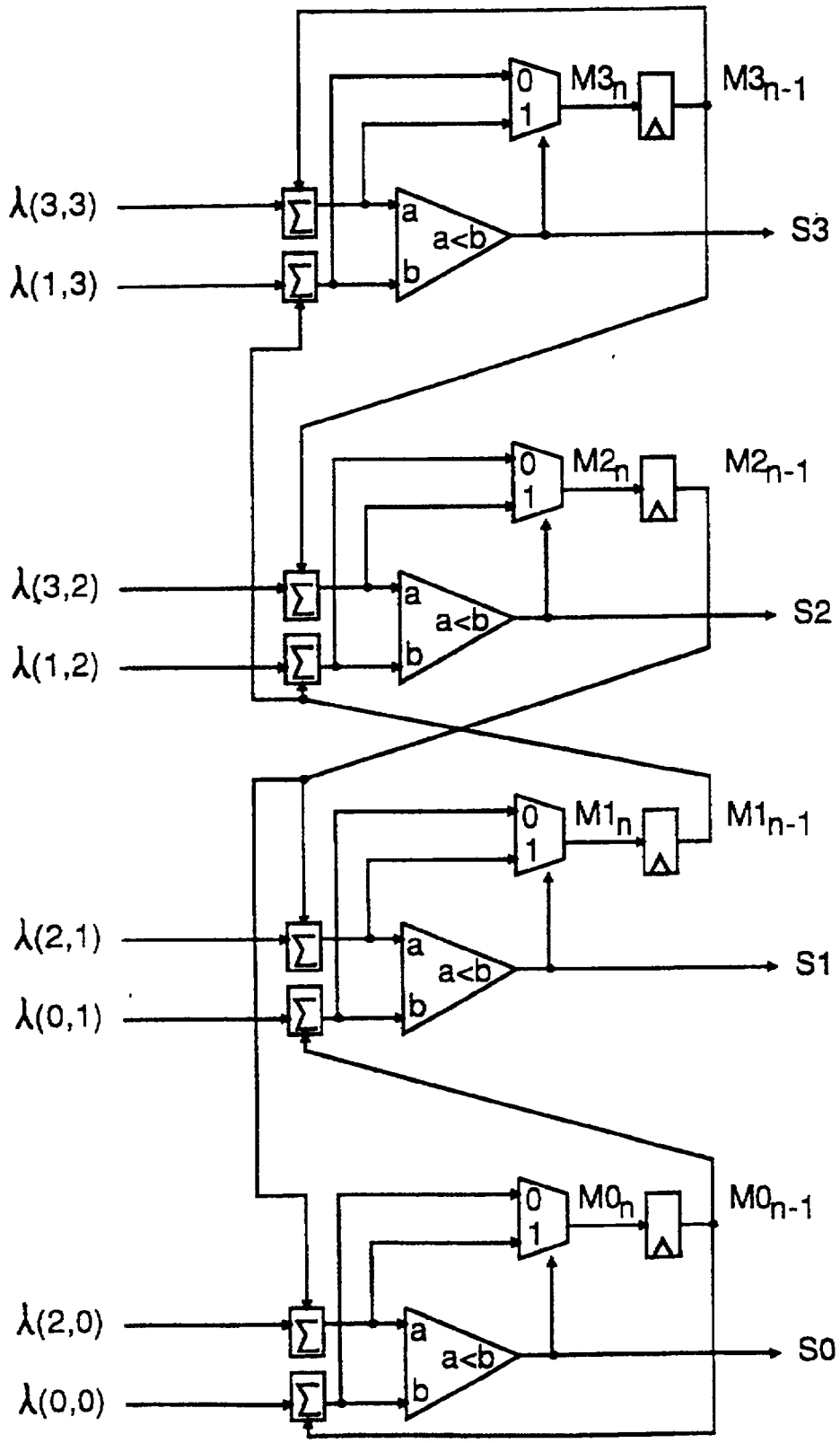

λ(3,3)
λ(1,3)
λ(3,2)
λ(1,2)
λ(2,1)
λ(0,1)
λ(2,0)
λ(0,0)
a
b
a<b
0
1
M3n
M3n-1
M2n
M2n-1
M1n
M1n-1
M0n
M0n-1
S3
S2
S1
S0

FIG. 17B

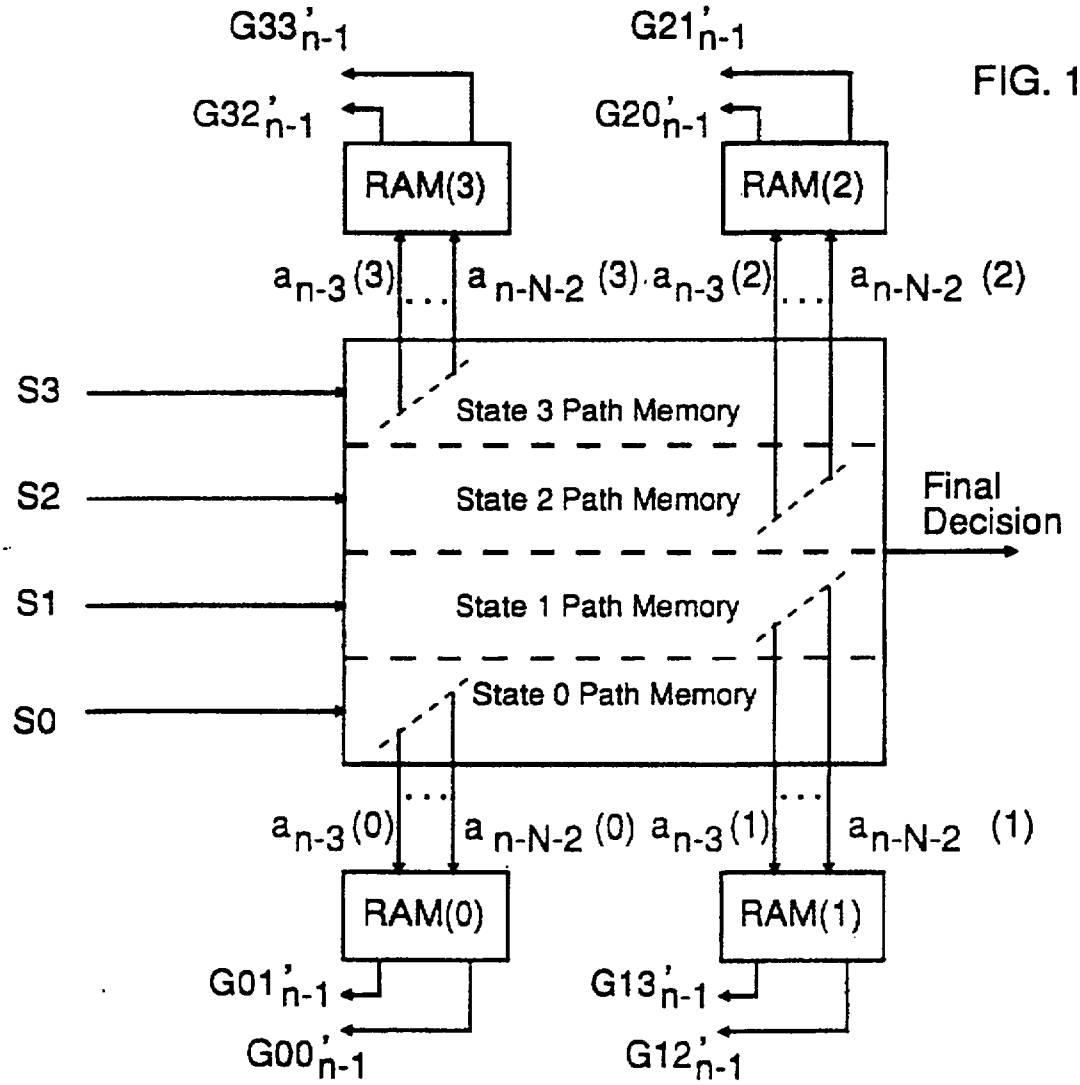

G33'n-1
G21'n-1
G32'n-1
G20'n-1
RAM(3)
RAM(2)
an-3 (3) ... an-N-2 (3) an-3 (2) ... an-N-2 (2)
S3
S2
S1
S0
State 3 Path Memory
State 2 Path Memory
State 1 Path Memory
State 0 Path Memory
Final Decision
an-3 (0) ... an-N-2 (0) an-3 (1) ... an-N-2 (1)
RAM(0)
RAM(1)
G01'n-1
G13'n-1
G00'n-1
G12'n-1

FIG. 17C

* C L M S *

Amended Claim

1. Apparatus for noise predictive maximum likelihood (NPML) sequence detection in a channel, comprising:

a. a prediction error filter for whitening colored random noise components of a sample y_n received via said channel, said sample y_n comprising a generalized partial-response signal component corrupted by said colored random noise components, leading to a signal z_n now having L intersymbol-interference components,

b. means for cancellation of K of said L intersymbol-interference components in said signal z_n, having

- a state complexity being equal to 2^K, with $0 \leq K \leq L$ and L reflecting the number of said intersymbol interference components, and
- survivor path means for storing path history decisions corresponding to 2^K survivor paths,

c. means for cancellation of L-K of said L intersymbol-interference components in said signal z_n, said means comprising

- feedback means for intersymbol-interference cancellation using precomputed and stored intersymbol-interference cancellation terms, and
- means for retrieving said intersymbol-interference cancellation terms by applying said path history decisions as addresses to said feedback means for intersymbol-interference cancellation.

AMENDED SHEET
IPEA/EP

REPLACEMENT SHEET
06 JAN 1998

RTMP COPY + IPER

PCT WORLD INTELLECTUAL PROPERTY ORGANIZATION
International Bureau

INTERNATIONAL APPLICATION PUBLISHED UNDER THE PATENT COOPERATION TREATY (PCT)

(51) International Patent Classification 6 : H04L 25/03, 25/497

A1

(11) International Publication Number: **WO 97/11544**

(43) International Publication Date: 27 March 1997 (27.03.97)

(21) International Application Number: PCT/IB95/00769

(22) International Filing Date: 18 September 1995 (18.09.95)

(71) Applicant: INTERNATIONAL BUSINESS MACHINES CORPORATION [US/US]; Old Orchard Road, Armonk, NY 10504 (US).

(72) Inventors: COKER, Jonathan, Darrel; 1605 5th Street Northeast, Rochester, MN 55901 (US). ELEFTHERIOU, Evangelos, Stavros; Bellariastrasse 53, CH-8038 Zürich (CH). GALBRAITH, Richard, Leo; 2232 N.W. 52nd Street, Rochester, MN 55901 (US). HIRT, Walter; Hinderweidstrasse 29, CH-8907 Wettswil (CH).

(74) Agent: BARTH, Carl, Otto; International Business Machines Corporation, Säumerstrasse 4, CH-8803 Rüschlikon (CH).

(81) Designated States: CN, JP, KR, SG, European patent (AT, BE, CH, DE, DK, ES, FR, GB, GR, IE, IT, LU, MC, NL, PT, SE).

Published
With international search report.

(54) Title: APPARATUS AND METHOD FOR NOISE-PREDICTIVE MAXIMUM-LIKELIHOOD (NPML) DETECTION

(57) Abstract

The present application makes use of a novel noise-predictive maximum-likelihood (NPML) data detection scheme (10) operating on signal samples received via an equalizing filter (22) from a channel, and in particular a storage channel of a direct access storage device. This scheme arises by applying a noise prediction/whitening process to the output signal of said equalizers and by providing means in the branch metric computation of a maximum-likelihood sequence detector (MLSD). It furthermore provides for cancellation of intersymbol-interference (ISI) components of said signal samples, by means of an appropriate table look-up. The contents of the table look-up are addressed by using decisions from the path histories of the maximum-likelihood sequence detector.

